Dynamic structure factor for the electron gas in metallic systems

F. Green, D. Neilson,* and J. Szymański
School of Physics, University of New South Wales, Kensington, Sydney 2033, Australia
(Received 14 September 1983)

A microscopic calculation is presented for the dynamic structure factor of the electron gas at metallic densities. The calculation is based on a theory of dynamic correlations in the electron gas, which is valid for high to metallic electron densities and which strictly maintains the conservation laws. A detailed comparison is made to the multiple peaks experimentally observed in the dynamic structure factors of Li and Be at momentum transfers greater than the Fermi momentum. From the quantitative agreement obtained, we conclude that the peak structures are a direct result of short-range Coulomb scattering correlations between two excited electrons. These correlations are frequency sensitive and highly nonlocal, and cannot be replicated by mean-field approximations.

I. INTRODUCTION

In the preceding paper[1] (to be referred to as I here) we formulated a new microscopic theory of correlations in the interacting electron gas at metallic densities. We incorporated in this theory a number of significant features.

(1) In the high-density limit of the electron gas, the theory reduces to the familiar random-phase approximation (RPA),[2] which is exact in this limit.

(2) At metallic densities and for large momentum transfers, our model reproduces the dominant correlations in the electron gas, namely, those due to strong short-range Coulomb scattering between two electrons.[3]

(3) At metallic densities and for small momentum transfers, our model includes correlations due to residual electron-hole screening, these being the leading corrections to the RPA high-density expansion.[4]

(4) The theory is applicable in all regimes of momentum and energy transfer and provides a unified framework for both dynamic and static correlation effects.

(5) The theory strictly conserves particle number, momentum, and energy. In particular, the dynamic structure factor exactly satisfies the f and conductivity sum rules.

In this paper we pursue the theory's predictions for the dynamic properties of the interacting electron gas at metallic densities and at large values of momentum transfer (that is, values greater than the Fermi momentum). For real metals (for example, Be, Al, Li) the dynamic structure factor, when plotted as a function of energy transfer, has been observed[5,6] to depart markedly from the prediction of the random-phase approximation (RPA) and its static mean-field generalizations.[7] We will present numerical calculations reinforcing our previous claim[8] that the intricate peak structure observed in the structure factor is a direct result of dynamic Coulomb-scattering correlations between electron pairs.

For a more extensive overview of existing approaches to the correlation problem in the electron gas, the reader is referred to the critical survey in paper I and to references therein.

In Sec. II we introduce the formalism and then present, in diagrammatic form, the structure of the correlation terms within our model. One class of terms in particular is distinguished by its sensitive dependence on the external energy transfer. Section III contains the detailed analysis of each class of contributions and the systematic formulation of a practical scheme for calculating the dynamic structure factor. Section IV presents our main numerical results for the structure factor. Finally, Sec. V contains concluding remarks.

II. DYNAMIC CORRELATIONS: FORMALISM

Section II A establishes notation and briefly reviews the main formal results of I. Section II B introduces the set of time-ordered correlation diagrams derived from our model. At large momentum transfers these diagrams fall naturally into three major groups.

A. General formulation

In this work we employ units such that $\hbar=m=1$. The Coulomb coupling constant e^2 is then equal to the inverse Bohr radius, $e^2=a_0^{-1}\approx 0.529$ Å^{-1}. Momentum is in units of inverse length, and energy has units of momentum squared. For an electron gas of particle density n, the Fermi momentum k_F is given by $k_F=(3\pi^2 n)^{1/3}\equiv(9\pi/4)^{1/3}a_0^{-1}r_s^{-1}$, where n has been expressed in terms of a_0^{-1} and the usual separation parameter r_s.

First, let us recall the relation between the total and proper polarization functions, $\chi(\vec{q},\omega)$ and $\chi^{sc}(\vec{q},\omega)$, for the uniform electron gas ($\vec{q}$ and ω are the momentum and energy transfers):

$$\chi(\vec{q},\omega)=\frac{\chi^{sc}(\vec{q},\omega)}{1-V(\vec{q})\chi^{sc}(\vec{q},\omega)} . \tag{1}$$

Here, $V(\vec{q})=4\pi e^2/q^2$ is the Fourier-transformed Coulomb interaction. The total polarization χ measures the response of the density to an arbitrary external potential in the weak-coupling limit, while the proper polarization χ^{sc} measures the density response to the total potential—the external potential plus the screening potential induced within the gas. The macroscopic dielectric

response of the system is completely determined by χ^{sc} through Eq. (1), and the structure of χ^{sc} depends only on the microscopic correlations in the system.

A quantity directly accessible in scattering experiments using a weakly coupled external probe is the dynamic structure factor $S(\vec{q},\omega)$. The relation between $S(\vec{q},\omega)$ and the proper polarization $\chi^{sc}(\vec{q},\omega)$ is

$$S(\vec{q},\omega)\equiv -\frac{1}{\pi}\mathrm{Im}\chi(\vec{q},\omega) = -\frac{1}{\pi}\frac{\mathrm{Im}\chi^{sc}(\vec{q},\omega)}{|1-V(\vec{q})\chi^{sc}(\vec{q},\omega)|^2} . \quad (2)$$

In I we applied the method of Baym and Kadanoff[9] to formulate a strictly conserving approximation for χ^{sc} by setting up a model of microscopic correlations via the following steps.

(i) We expressed the exact ground-state energy of the interacting system as a functional of the fully dressed one-body propagator $\underline{G}$.

(ii) From the complete set of closed Feynman diagrams representing the exchange-correlation part of this energy functional, we retained a subset (Fig. 1) with the following characteristics.

(a) The subset included all particle-particle Coulomb scattering "ladder" diagrams, which dominate the large-momentum correlation contribution.[3]

(b) The subset included all particle-hole polarization "ring" diagrams, which dominate the screening correlations at small momenta.

(c) Within each given diagram of our subset, every propagator $\underline{G}$ was equivalent to every other $\underline{G}$ in the diagram. This symmetry preserves the space-time invariant form of the energy functional, thereby ensuring conservation.[1]

(iii) By formally minimizing the symmetric functional for the ground-state energy with respect to $\underline{G}$, we generated an approximate but strictly conserving one-body equation of motion, allowing us in principle to evaluate the propagator $\underline{G}$ in a self-consistent way:

$$G^{-1}(\vec{k},k^0)=[G^{(0)}(\vec{k},k^0)]^{-1}-\Sigma[\underline{G}](\vec{k},k^0) . \quad (3)$$

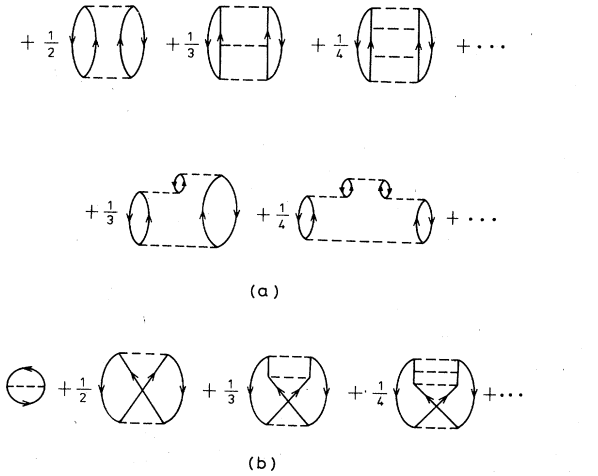

FIG. 1. Contributions to the exchange-correlation component of the ground-state energy functional $\Phi[\underline{G}]$ within our model. The accompanying fractions are weighting factors, and there is an implicit overall factor of $\frac{1}{2}$. Solid lines indicate the self-consistent particle propagators $\underline{G}$ in the Feynman representation. (a) Direct scattering ladder plus ring diagrams. (b) Hartree-Fock plus exchange ladder diagrams.

The $\vec{k}$ and k^0 are the momentum and energy variables for a single particle, and $G^{(0)}(\vec{k},k^0)=(k^0-k^2/2)^{-1}$ is the single-particle propagator for the noninteracting electron gas. The functional $\underline{\Sigma}[\underline{G}]$ is our single-particle self-energy. It is defined as the variational derivative of the ground-state energy functional with respect to $(-i\underline{G})$.

(iv) Finally, by taking the second variation with respect to $\underline{G}$ of the ground-state energy functional, we generated a conserving integral equation for the proper electron-hole polarization propagator which we denoted by $\underline{\Lambda}^{sc}[\underline{G}]$. The equation for $\underline{\Lambda}^{sc}[\underline{G}]$ contains an effective two-body interaction, $\underline{\Xi}^{sc}[\underline{G}]$. This interaction explicitly exhibits within its diagrammatic expansion all the microscopic dynamical correlations which are implicit in our choice of a conserving energy functional. The equation for $\underline{\Lambda}^{sc}[\underline{G}]$ is

$$\Lambda^{sc}[\underline{G}](\vec{k}_1,k_1^0;\vec{q},\omega)=-iG(\vec{k}_1,k_1^0)G(\vec{q}+\vec{k}_1,\omega+k_1^0) \times\left[1+\sum_{\vec{k}_2,\sigma_2}\int\frac{dk_2^0}{2\pi i}\{\Xi^{sc}[\underline{G}]_{\sigma_1\sigma_2}(\vec{k}_1,k_1^0;\vec{k}_2,k_2^0;\vec{q},\omega)\}\{\Lambda^{sc}[\underline{G}](\vec{k}_2,k_2^0;\vec{q},\omega)\}\right] . \quad (4)$$

Here $(\vec{k}_1,\sigma_1,k_1^0)$ and $(\vec{k}_2,\sigma_2,k_2^0)$ are single-particle variables. Although $\underline{\Lambda}^{sc}[\underline{G}]$ does not depend on spin σ, the effective interaction $\underline{\Xi}^{sc}[\underline{G}]$ includes exchange processes and these contributions carry a Kronecker factor $\delta_{\sigma_1,\sigma_2}$. The proper polarization function χ^{sc} is simply the trace of $\underline{\Lambda}^{sc}[\underline{G}]$ over its single-particle label:

$$\chi^{sc}(\vec{q},\omega)=\sum_{\vec{k}_1,\sigma_1}\int\frac{dk_1^0}{2\pi i}\Lambda^{sc}[\underline{G}](\vec{k}_1,k_1^0;\vec{q},\omega) . \quad (5)$$

Steps (i)—(iv), together with the diagrams for the ground-state energy functional (Fig. 1), uniquely define our model.

We may expand $\underline{\Lambda}^{sc}[\underline{G}]$ in Eq. (5) in powers of $\underline{\Xi}^{sc}[\underline{G}]$. For χ^{sc} we obtain a series of terms $\chi^0,\chi^1,\chi^2,\ldots$ of increasing order in the effective interaction. To first order in $\underline{\Xi}^{sc}[\underline{G}]$ we have

$$\chi^{sc}(\vec{q},\omega)\approx\chi^{0}(\vec{q},\omega)+\chi^{1}(\vec{q},\omega)\ ,$$

$$\chi^{0}(\vec{q},\omega)=2\sum_{\vec{k}_1}\int\frac{dk_1^0}{2\pi i}G(\vec{k}_1,k_1^0)G(\vec{q}+\vec{k}_1,\omega+k_1^0)\ ,$$

$$\chi^{1}(\vec{q},\omega)=4\sum_{\vec{k}_1}\sum_{\vec{k}_2}\int\frac{dk_1^0}{2\pi i}\int\frac{dk_2^0}{2\pi i}G(\vec{k}_1,k_1^0)G(\vec{q}+\vec{k}_1,\omega+k_1^0)\left[\frac{1}{4}\sum_{\sigma_1,\sigma_2}\{\Xi^{sc}[\underline{G}]_{\sigma_1\sigma_2}(\vec{k}_1,k_1^0;\vec{k}_2,k_2^0;\vec{q},\omega)\}\right]$$

$$\times G(\vec{k}_2,k_2^0)G(\vec{q}+\vec{k}_2,\omega+k_2^0)\ . \tag{6}$$

The leading term $\chi^0(\vec{q},\omega)$ represents the propagation of a renormalized particle and a renormalized hole without mutual correlations. In the high-density limit this function reduces to the familiar Lindhard function.[2] The next term, $\chi^1(\vec{q},\omega)$, contains to lowest order all the pair correlations built into $\Xi^{sc}[\underline{G}]$. To examine these pair correlations we now evaluate $\chi^1(\vec{q},\omega)$.

B. Diagrammatic expansion for χ^1

After the frequency integrals in the Feynman diagrams have been performed, the polarization function $\chi^1(\vec{q},\omega)$ in Eq. (6) becomes the sum of all possible time-ordered Goldstone diagrams.[10] Correspondingly $\Xi^{sc}[\underline{G}]$ separates out into a set of scattering matrix elements linking the initial and final particle-hole pairs of χ^1. Each of these matrix elements can be expanded in terms of the components of either the T matrix ($\underline{T}$) or the shielded potential ($\underline{V}^{sc}$); there is no mixing of $\underline{T}$ terms and $\underline{V}^{sc}$ terms within Ξ^{sc}. Figure 2 defines the T matrix and the shielded-potential interactions.

In Figs. 3–9 we show the time-ordered diagrams for $\chi^1(\vec{q},\omega)$. The corresponding Feynman diagrams for χ^1 may be found in Fig. 4 of paper I. As usual forward-propagating particle lines (electrons) have an arrow pointing up, while backward-propagating lines (holes) point down. In each diagram of these figures we use a pair of solid horizontal lines to schematically represent two components in the series expansion for either $\underline{T}$ or $\underline{V}^{sc}$ (both components will belong to the same series). Two such horizontal lines delineate the start and end of a given dynamical correlation process in $\Xi^{sc}[\underline{G}]$. Figures 3–6 show those terms for which the pair of $\underline{T}$ or $\underline{V}^{sc}$ interactions do not overlap in time. We defer discussion of the overlapping terms. The time-ordered contributions to χ^1 fall into four classes, A through D. We discuss here the first three classes (Figs. 3 through 8).

Class A (Fig. 3). Contributions in which the initial and final electron-hole pairs both carry the external momentum and energy $(\vec{q},\omega)$ in the same time direction. At large $(\vec{q},\omega)$ this implies large transfers of momentum and energy from the initial to the final pair, resulting in on-shell scattering between these forward-propagating pairs.

Class B (Figs. 4 and 5). Contributions in which the initial and final electron-hole pairs propagate in opposite time directions. At large $(\vec{q},\omega)$ these terms retain a net momentum transfer of order $\vec{q}$ between the pairs, but there is no overall energy transfer; they consequently represent purely static correlations.

Class C (Figs. 6 to 8). Contributions in which the initial and final pairs propagate in the same time direction but such that the correlations link electron and hole. Because of the strong phase-space constraints for this class, the transfer of energy and momentum within the interaction is very restricted even for large $\vec{q}$. When $\vec{q}$ is large, the transfer is either limited to be of the order of the Fermi energy E_F and Fermi momentum k_F, respectively, or else there may be at most one outer interaction line which transfers momentum $\sim\vec{q}$, while all the other bare interaction lines transfer momentum $\lesssim k_F$.

The main objective of our present analysis is to demonstrate that the class-A group dominates the fine-scale ω behavior of the dynamic structure factor $S(\vec{q},\omega)$. For

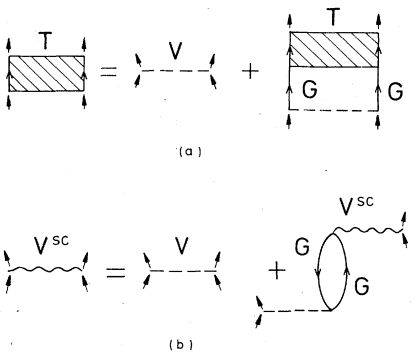

FIG. 2. Definition of the T matrix with self-consistent propagators. Each pair $\underline{G}\,\underline{G}$ is either electron-electron or hole-hole. (b) Definition of $\underline{V}^{sc}$, the dynamically shielded RPA interaction with self-consistent electron and hole propagators $\underline{G}$.

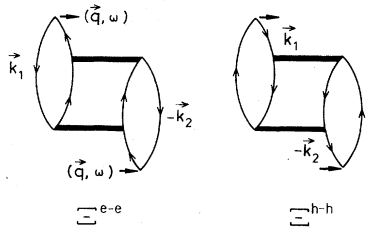

FIG. 3. Class-A contributions to $\chi^1(\vec{q},\omega)$ for which the initial and final electron-hole pairs both transport the external momentum and energy in the same time direction. In this and succeeding figures the time-ordered (Goldstone) representation is used.

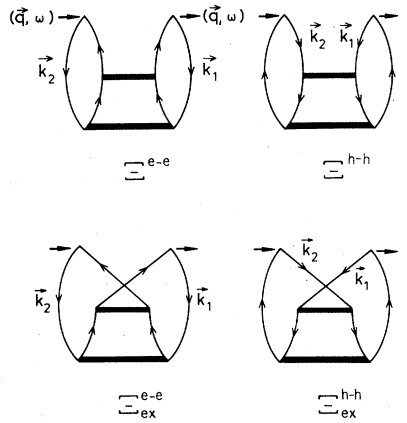

FIG. 4. Class-B contributions to $\chi^1(\vec{q},\omega)$ involving electron-electron or hole-hole correlations. In this class initial and final electron-hole pairs propagate in opposite time directions.

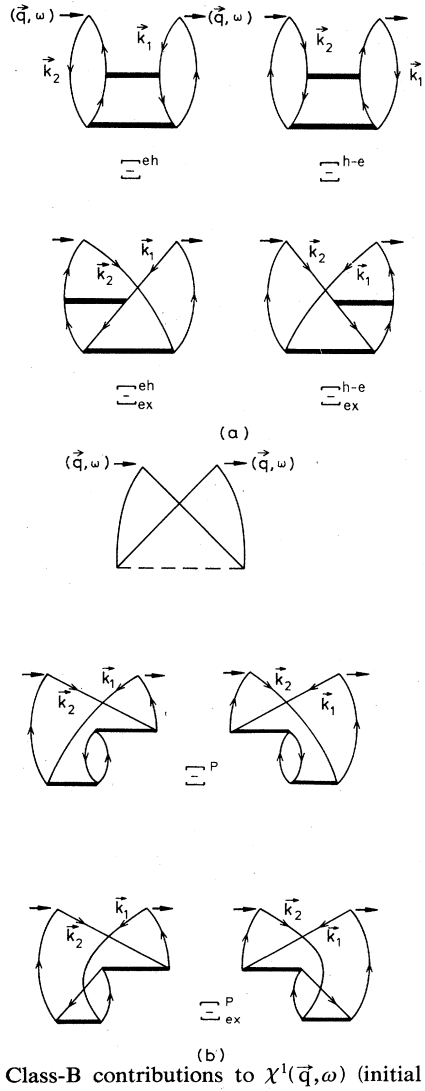

FIG. 5. Class-B contributions to $\chi^1(\vec{q},\omega)$ (initial and final electron-hole pairs propagating in opposite time directions) in which the correlation is between electron and hole. (a) Electron-hole two-pair correlations. (b) Electron-hole one-pair correlations.

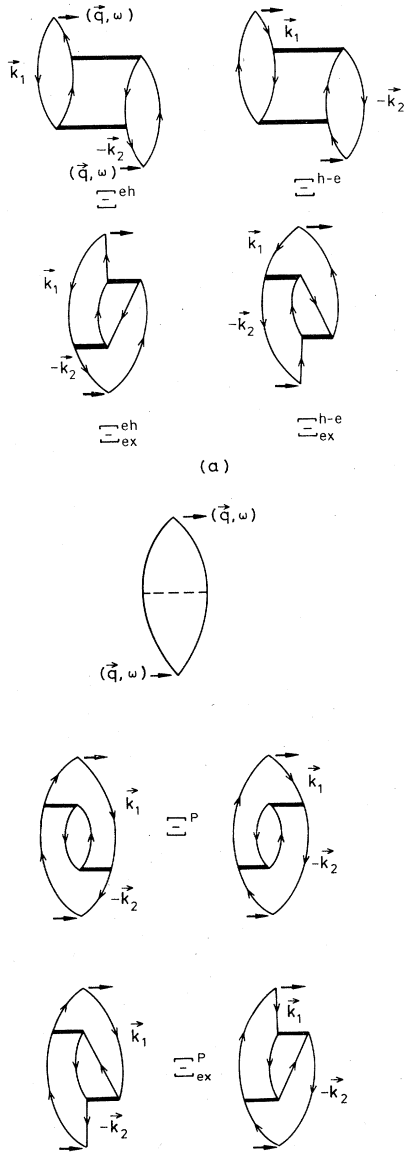

FIG. 6. Class-C contributions to $\chi^1(\vec{q},\omega)$ for which the initial and final electron-hole pairs propagate in the same time direction and in which the correlations are between electron and hole. (a) Electron-hole two-pair correlations. (b) Electron-hole one-pair correlations.

convenience we have labeled the parts of $\Xi^{sc}[\underline{G}]$ in Figs. 3—9 as follows.

$\Xi^{e\text{-}e}$: all interactions in Ξ^{sc} involving the propagation of two intermediate excited electrons at all times between the initial and final scatterings.

$\Xi^{h\text{-}h}$: all interactions in Ξ^{sc} involving at least one intermediate hole-hole excitation.

The two contributions above will be denoted generically by $\Xi^{p\text{-}p}$.

$\Xi^{e\text{-}h}$, $\Xi^{h\text{-}e}$: all interaction ladders in Ξ^{sc} involving the intermediate scattering of an electron and a hole.

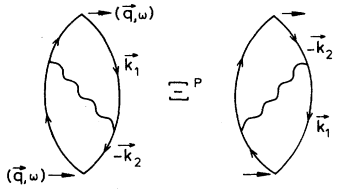

FIG. 7. Class-C contributions to $\chi^1(\vec{q},\omega)$ in which the single electron-hole pair is correlated through the full dynamically screened interaction $\underline{V}^{sc}$.

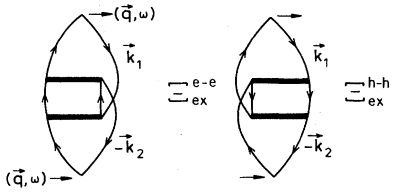

FIG. 8. Class-C contributions to $\chi^1(\vec{q},\omega)$ comprising the exchange terms for the electron-electron and hole-hole correlation terms shown in Fig. 3.

We will refer to electron-hole interactions generically as $\underline{\Xi}^{p\text{-}\bar{p}}$.

$\underline{\Xi}^{P}$: all interactions in $\underline{\Xi}^{sc}$ with at least one intermediate electron-hole polarization bubble.

Where appropriate the analogs of these composite interactions, produced by exchanging two particle lines, will be distinguished by the subscript ex, as for example in $\underline{\Xi}^{e\text{-}e}_{ex}$.

Having introduced the family of terms that make up $\underline{\Xi}^{sc}$, we now examine their functional behavior.

III. DYNAMIC CORRELATIONS: ANALYSIS

This section consists of three parts, in the first of which we write explicit expressions for the classes A, B, and C introduced in the preceding section. A fourth class, D, involving two-plasmon scattering is introduced. Of the four classes, only the class-A terms have a structure which leads to rapidly varying dynamical behavior. Section III B discusses self-energy insertions in the single-particle propagators. It is shown that such insertions, when consistently treated in the time-ordered diagram representation, cannot contribute to the rapid variation of $\chi^{sc}(\vec{q},\omega)$ with the energy ω. Finally in Sec. III C we combine the results of our diagrammatic analysis with some formal techniques from paper I to produce a tractable scheme for calculating $\chi^{sc}(\vec{q},\omega)$. This scheme reveals important and novel dynamic effects.

A. Structure of $\underline{\Xi}^{sc}$

In $\chi^1(\vec{q},\omega)$ the parts of $\underline{\Xi}^{sc}[\underline{G}]$ act effectively as two-body matrix elements which couple the initial electron-hole polarization pair propagator to the final pair propagator. These matrix elements are in general nonlocal since they depend on the outer hole momenta $\vec{k}_1,\vec{k}_2$ as well as on $\vec{q}$. They are also energy dependent since they vary with the outer electron and hole energies as well as with ω. We will express the matrix elements of $\underline{\Xi}^{p\text{-}p}[\underline{G}]$, $\underline{\Xi}^{p\text{-}\bar{p}}[\underline{G}]$, and $\underline{\Xi}^{P}[\underline{G}]$ in the form $\langle \vec{Q}_{out} | \Xi(\vec{P},E) | \vec{Q}_{in} \rangle$, where (i) $\vec{P}$ is the total conserved momentum of the attached (incoming or outgoing) fermion lines, (ii) E is the net energy input from the attached fermion lines (this can be straightforwardly determined from the rules for Goldstone diagrams[10]), and (iii) $\vec{Q}_{out}$ and $\vec{Q}_{in}$ are the outgoing and incoming relative momenta of the attached fermion lines.

To simplify the discussion here we will replace all dressed propagators $\underline{G}$ in the diagrams of Figs. 3–8 with their bare counterparts $\underline{G}^{(0)}$; our justification for this step can be found in Sec. III B.

1. Class A

We can write the class-A contributions to $\chi^1(\vec{q},\omega)$ (see Fig. 3) as

$$\chi^{A}(\vec{q},\omega)\equiv 4\sum_{\vec{k}_1}\frac{\Theta^{<}_{\vec{k}_1}\Theta^{>}_{\vec{q}+\vec{k}_1}}{E_1(\omega)}\sum_{\vec{k}_2}\frac{\Theta^{<}_{\vec{k}_2}\Theta^{>}_{\vec{q}-\vec{k}_2}}{E_2(\omega)} \times\Xi^{A}(\vec{k}_1,-\vec{k}_2;\vec{q},\omega)\,. \tag{7}$$

Our notation is as follows. The outer electron-hole pair energy denominators are defined as

$$E_1(\omega)\equiv\omega-\epsilon^{(0)}_{\vec{q}+\vec{k}_1}+\epsilon^{(0)}_{\vec{k}_1}+i\eta\,,$$
$$E_2(\omega)\equiv\omega-\epsilon^{(0)}_{\vec{q}-\vec{k}_2}+\epsilon^{(0)}_{\vec{k}_2}+i\eta\,, \tag{8}$$

where $\epsilon^{(0)}_{\vec{p}}=p^2/2$ is the bare single-particle energy for a particle of momentum $\vec{p}$, and $\eta=0^+$. The Fermi cutoff functions $\Theta^{<}_{\vec{p}},\Theta^{>}_{\vec{p}}$ are defined in terms of the usual step function $\Theta(x)=(x+|x|)/2|x|$:

$$\Theta^{<}_{\vec{p}}=\Theta(k_F-p)\,,$$
$$\Theta^{>}_{\vec{p}}=\Theta(p-k_F)\,. \tag{9}$$

The class-A-type interaction $\Xi^{A}(\vec{k}_1,-\vec{k}_2;\vec{q},\omega)$ is the spin-averaged sum of $\underline{\Xi}^{e\text{-}e}$ and $\underline{\Xi}^{h\text{-}h}$. We have

$$\Xi^{A}(\vec{k}_1,-\vec{k}_2;\vec{q},\omega)=\langle\tfrac{1}{2}(\vec{K}+\vec{q})\,|\,\Xi^{e\text{-}e}(\vec{\mathcal{K}},\omega+\epsilon^{(0)}_{\vec{k}_1}+\epsilon^{(0)}_{\vec{k}_2})\,|\,\tfrac{1}{2}(\vec{K}-\vec{q})\rangle$$
$$+\langle\tfrac{1}{2}(\vec{K}+\vec{q})\,|\,\Xi^{h\text{-}h}(\vec{\mathcal{K}},\omega-\epsilon^{(0)}_{\vec{q}+\vec{k}_1}-\epsilon^{(0)}_{\vec{q}-\vec{k}_2})\,|\,\tfrac{1}{2}(\vec{K}-\vec{q})\rangle\,. \tag{10}$$

Momentum variables are given in terms of $\vec{k}_1, \vec{k}_2$, and $\vec{q}$ by $\vec{K}=\vec{k}_1+\vec{k}_2$ and $\vec{\mathcal{K}}=\vec{q}+2\vec{k}$, where $\vec{k}=(\vec{k}_1-\vec{k}_2)/2$.

The leading terms of Ξ^{A} expanded as Born series in powers of the Coulomb potential V are of second order in V. These leading-order terms already display the functional behavior of all particle-particle excitations, and it is instructive to look at the second-order Born terms explicitly:

$$\Xi_2^{e\text{-}e\,A}=\sum_{\vec{p}} V(\vec{Q}_1)\frac{\Theta^{>}_{\vec{p}_1}\Theta^{>}_{\vec{p}_2}}{\frac{1}{2}[E_1(\omega)+E_2(\omega)]+\frac{1}{4}(q^2+K^2)-p^2}V(\vec{Q}_2)\,, \tag{11a}$$

and

$$\Xi_2^{h\text{-}h\,A}=\sum_{\vec{p}} V(\vec{Q}_1)\frac{\Theta^{<}_{\vec{p}_1}\Theta^{<}_{\vec{p}_2}}{\frac{1}{2}[E_1(\omega)+E_2(\omega)]-\frac{1}{4}(q^2+K^2)+p^2}V(\vec{Q}_2)\,, \tag{11b}$$

where $\vec{p}_1=\frac{1}{2}\vec{\mathcal{K}}+\vec{p}$, $\vec{p}_2=\frac{1}{2}\vec{\mathcal{K}}-\vec{p}$, $\vec{Q}_1=\frac{1}{2}(\vec{K}+\vec{q})-\vec{p}$, and $\vec{Q}_2=\vec{p}-\frac{1}{2}(\vec{K}-\vec{q})$. The outer particle-hole energies $E_1(\omega)$ and $E_2(\omega)$ are as in Eq. (8). In their more familiar form, the intermediate energy denominators are

$$\omega+\epsilon^{(0)}_{\vec{k}_1}+\epsilon^{(0)}_{\vec{k}_2}-\epsilon^{(0)}_{\vec{p}_1}-\epsilon^{(0)}_{\vec{p}_2}=\tfrac{1}{2}[E_1(\omega)+E_2(\omega)]+[\tfrac{1}{4}(q^2+K^2)-p^2]\,, \tag{12a}$$

$$\omega-\epsilon^{(0)}_{\vec{q}+\vec{k}_1}-\epsilon^{(0)}_{\vec{q}-\vec{k}_2}+\epsilon^{(0)}_{\vec{p}_1}+\epsilon^{(0)}_{\vec{p}_2}=\tfrac{1}{2}[E_1(\omega)+E_2(\omega)]-[\tfrac{1}{4}(q^2+K^2)-p^2]\,. \tag{12b}$$

In Eq. (11a) we have a singular interaction which peaks for $\vec{p}^{\,2}=\frac{1}{4}(\vec{q}^{\,2}+\vec{K}^{\,2})+\frac{1}{2}\vec{q}\cdot\vec{K}$, and another interaction which peaks for $\vec{p}^{\,2}=\frac{1}{4}(\vec{q}^{\,2}+\vec{K}^{\,2})-\frac{1}{2}\vec{q}\cdot\vec{K}$. These two peaks are thus separated by $\Delta p^2\sim qk_F$. The divergences in the interactions are cut off by the Pauli operators, which nevertheless permit large contributions from the peaks. A singular energy denominator is sandwiched in between the peaks. At the center of the single-particle excitation region we have $\omega\approx\frac{1}{2}q^2$, so that $\frac{1}{2}\,|E_1(\omega)+E_2(\omega)|\lesssim qk_F$. The energy denominator of Eq. (11a) goes through zero when $\vec{p}^{\,2}\approx\frac{1}{4}(\vec{q}^{\,2}+\vec{K}^{\,2})$, i.e., directly between the two interaction peaks. Consequently, following the summation over $\vec{p}$ in Eq. (11a), $\Xi^{e\text{-}e\,A}$ will exhibit a rapidly varying peak-and-dip structure on a scale $\Delta\omega\sim qk_F$ when ω is in the region of single-particle excitations (i.e., $|\omega-q^2/2|\lesssim qk_F$). This ultimately leads to fine ω structure, on a similar $\Delta\omega$ scale, within the central peak of the structure factor $S(\vec{q},\omega)$.

In order to assess the contribution to $\chi^{A}(\vec{q},\omega)$ of hole-hole scattering correlations we first note that the Pauli projection operator for hole states severely restricts the available phase space when the momentum transfer $\vec{q}$ is large. Although the energy denominator for hole scattering [Eq. (12b)] can vanish in an accessible region of phase space, the relative hole momentum $\vec{p}$ must be such that

$$p^2\lesssim k_F^2-\tfrac{1}{4}q^2-k^2+O(qk_F) \tag{13a}$$

and

$$p^2\sim\tfrac{1}{4}(q^2+K^2)+O(qk_F)\,. \tag{13b}$$

Even under the least stringent choice of the hole parameters $\vec{K}$ and $\vec{k}$, these two requirements almost exclude each other for $q>2k_F$. We conclude that dynamic hole-hole scattering at large momenta is negligible in comparison with electron-electron scattering.

2. *Class B*

The class-B terms of $\chi^1(\vec{q},\omega)$ are defined in Figs. 4 and 5. They all contain initial and final electron-hole pairs which propagate in opposite time directions and therefore overlap in the time domain without restriction. Their mutual correlations are thus static. This is reflected in the absence of the external energy ω in all intermediate energy denominators. However, the momentum transfer between the initial and final pairs is always close to the external momentum $\vec{q}$ when $\vec{q}$ is large. The class-B contributions to χ^1 are denoted by χ^{B}:

$$\chi^{B}(\vec{q},\omega)=4\sum_{\vec{k}_1}\frac{\Theta^{<}_{\vec{k}_1}\Theta^{>}_{\vec{q}+\vec{k}_1}}{E_1(\omega)}\sum_{\vec{k}_2}\frac{\Theta^{<}_{\vec{k}_1}\Theta^{>}_{\vec{k}_2-\vec{q}}}{E_2(-\omega)}\times\Xi^{B}(\vec{k}_1,\vec{k}_2;\vec{q},\omega)\,. \tag{14}$$

The spin-averaged interaction Ξ^{B} can be divided into particle-particle terms $\Xi^{p\text{-}p}$ and electron-hole terms, $\Xi^{p\text{-}\bar{p}}$ and Ξ^{P}. The $\Xi^{p\text{-}p}$ group, including fermion exchange, is

$$\Xi^{p\text{-}p\,B}(\vec{k}_1,\vec{k}_2;\vec{q},\omega)=\langle\vec{q}+\vec{k}\,|\,\Xi^{e\text{-}e}(\vec{K},\epsilon^{(0)}_{\vec{k}_1}+\epsilon^{(0)}_{\vec{k}_2})\,|\,\vec{k}\rangle+\langle\vec{q}+\vec{k}\,|\,\Xi^{h\text{-}h}(\vec{K},-\epsilon^{(0)}_{\vec{q}+\vec{k}_1}-\epsilon^{(0)}_{\vec{k}_2-\vec{q}})\,|\,\vec{k}\rangle$$
$$-\tfrac{1}{2}\langle\vec{q}+\vec{k}\,|\,\Xi^{e\text{-}e}(\vec{K},\epsilon^{(0)}_{\vec{k}_1}+\epsilon^{(0)}_{\vec{k}_2})\,|\,-\vec{k}\rangle-\tfrac{1}{2}\langle\vec{q}+\vec{k}\,|\,\Xi^{h\text{-}h}(\vec{K},-\epsilon^{(0)}_{\vec{q}+\vec{k}_1}-\epsilon^{(0)}_{\vec{k}_2-\vec{q}})\,|\,-\vec{k}\rangle\,. \tag{15}$$

The momenta $\vec{K}$ and $\vec{k}$ are as previously defined for Eq. (10), and we have expressed the matrix elements for $\Xi^{p\text{-}p}_{ex}$ in terms of $\Xi^{p\text{-}p}$. We again discuss the functional form of $\Xi^{p\text{-}p\,B}$ by examining its second-order Born terms:

$$(\Xi^{e\text{-}e}+\Xi^{e\text{-}e}_{ex})^{B}_{2}=\sum_{\vec{p}} V(\vec{q}+\vec{k}-\vec{p})\frac{\Theta^{>}_{\vec{p}_1},\Theta^{>}_{\vec{p}_2},}{k^2-p^2}[V(\vec{p}-\vec{k})-\tfrac{1}{2}V(\vec{p}+\vec{k})]\,, \tag{16a}$$

$$(\Xi^{h\text{-}h}+\Xi^{h\text{-}h}_{ex})^{B}_{2}=\sum_{\vec{p}} V(\vec{q}+\vec{k}-\vec{p})\frac{\Theta^{<}_{\vec{p}_1},\Theta^{<}_{\vec{p}_2},}{p^2-|\vec{q}+\vec{k}|^2}[V(\vec{p}-\vec{k})-\tfrac{1}{2}V(\vec{p}+\vec{k})]\,. \tag{16b}$$

Here $\vec{p}\,'_1=\frac{1}{2}\vec{K}+\vec{p}$ and $\vec{p}\,'_2=\frac{1}{2}\vec{K}-\vec{p}$ are the momenta of the intermediate excited particle pairs. The original forms of the energy denominators are

$$k^2-p^2=\epsilon^{(0)}_{\vec{k}_1}+\epsilon^{(0)}_{\vec{k}_2}-\epsilon^{(0)}_{\vec{p}\,'_1}-\epsilon^{(0)}_{\vec{p}\,'_2}\,, \tag{17a}$$

and

$$p^2-|\vec{q}+\vec{k}\,|^2=\epsilon^{(0)}_{\vec{p}\,'_1}+\epsilon^{(0)}_{\vec{p}\,'_2}-\epsilon^{(0)}_{\vec{q}+\vec{k}_1}-\epsilon^{(0)}_{\vec{q}+\vec{k}_2}\,. \tag{17b}$$

Note, in contrast with Eqs. (12a) and (12b), that these energy denominators are independent of ω and negative definite (because of the Pauli restrictions), and consequently lead to purely static correlations.

It is known from previous work[3] that $\Xi^{p\text{-}pB}$ is a slowly varying function of the outer hole momenta $\vec{k}_1$ and $\vec{k}_2$ and is consequently well approximated by its local average over hole states. We again stress that this property is not shared by the corresponding class-A term which, as we have seen, is strongly nonlocal. The denominator for $\Xi^{h\text{-}hB}$ is of order q^2 for large $\vec{q}$ so that $|\Xi^{h\text{-}hB}/\Xi^{e\text{-}eB}|$ is at most of order $(k_F/q)^2$, and is negligible to this order.

The electron-hole contributions to Ξ^{B} have the general forms

$$\Xi^{p\text{-}\bar{p}B}(\vec{k}_1,\vec{k}_2;\vec{q},\omega)=2\langle\tfrac{1}{2}(\vec{K}+\vec{q})\,|\,\Xi^{e\text{-}h}(\vec{\mathscr{K}},\epsilon^{(0)}_{\vec{k}_1}-\epsilon^{(0)}_{\vec{k}_2-\vec{q}})\,|\,\tfrac{1}{2}(\vec{K}-\vec{q})\rangle-\langle\tfrac{1}{2}(\vec{K}+\vec{q})\,|\,\Xi^{e\text{-}h}_{ex}(\vec{\mathscr{K}},\epsilon^{(0)}_{\vec{k}_1}-\epsilon^{(0)}_{\vec{k}_2-\vec{q}})\,|\,\tfrac{1}{2}(\vec{K}-\vec{q})\rangle, \tag{18a}$$

$$\Xi^{PB}(\vec{k}_1,\vec{k}_2;\vec{q},\omega)=-\tfrac{1}{2}[V(\vec{\mathscr{K}})+2\langle\vec{q}+\vec{k}\,|\,\Xi^{P}(\vec{K},\epsilon^{(0)}_{\vec{k}_1}-\epsilon^{(0)}_{\vec{k}_2-\vec{q}})\,|\,-\vec{k}\rangle-\langle\vec{q}+\vec{k}\,|\,\Xi^{P}_{ex}(\vec{K},\epsilon^{(0)}_{\vec{k}_1}-\epsilon^{(0)}_{\vec{k}_2-\vec{q}})\,|\,-\vec{k}\rangle]\,. \tag{18b}$$

We have exploited the symmetry of χ^{B} under the transformation $\vec{k}_1,\omega\rightleftarrows(-\vec{k}_2,-\omega)$ to combine $\Xi^{e\text{-}h}$ and $\Xi^{h\text{-}e}$, etc. The explicit functional forms of $\Xi^{p\text{-}\bar{p}B}$ and Ξ^{PB} can be illustrated by writing out their second-order Born terms:

$$(\Xi^{e\text{-}h}+\Xi^{e\text{-}h}_{ex})^{B}_{2}=\sum_{\vec{p}} V(\tfrac{1}{2}(\vec{K}+\vec{q})-\vec{p})\frac{\Theta^{<}_{-\vec{p}_2}\Theta^{>}_{\vec{p}_1}}{\vec{\mathscr{K}}\cdot[\frac{1}{2}(\vec{K}-\vec{q})-\vec{p}\,]}[V(\vec{p}-\tfrac{1}{2}(\vec{K}-\vec{q}))-\tfrac{1}{2}V(\vec{\mathscr{K}})] \tag{19a}$$

and

$$(\Xi^{P}+\Xi^{P}_{ex})^{B}_{2}=-\tfrac{1}{2}\sum_{\vec{p}} V(\vec{\mathscr{K}})\frac{\Theta^{<}_{-\vec{p}_2}\Theta^{>}_{\vec{p}_1}}{\vec{\mathscr{K}}\cdot[\frac{1}{2}(\vec{K}-\vec{q})-\vec{p}]}[V(\vec{\mathscr{K}})-\tfrac{1}{2}V(\vec{p}-\tfrac{1}{2}(\vec{K}-\vec{q}))]\,. \tag{19b}$$

The energy denominators are independent of the external energy ω [compare Eqs. (16)], and remain negative in the allowed region of phase space. When $\vec{q}$ is large the Pauli operators have two effects: (i) they force the energy denominators to be of order q^2, and (ii) the interactions in brackets in Eqs. (19a) and (19b) always carry a momentum of order $\vec{q}$. Consequently $\Xi^{p\text{-}\bar{p}B}$ is of order $(k_F/q)^2$ smaller than $\Xi^{e\text{-}eB}$, and Ξ^{PB}, which contains an additional interaction with momentum approximately equal to $\vec{q}$, is of order $(k_F/q)^4$ smaller than $\Xi^{e\text{-}eB}$.

We conclude that the leading contributions to Ξ^{B} are the lowest-order Hartree-Fock term plus the electron-electron scattering term $\Xi^{e\text{-}eB}$, both of which are of order $V(\vec{q})$.

3. *Class C*

Figures 6–8 show the contributions to $\chi^{C}(\vec{q},\omega)$. The terms in Fig. 6 can be written as

$$\chi'^{C}(\vec{q},\omega)=4\sum_{\vec{k}_1}\frac{\Theta^{<}_{\vec{k}_1}\Theta^{>}_{\vec{q}+\vec{k}_1}}{E_1(\omega)}\sum_{\vec{k}_2}\frac{\Theta^{<}_{\vec{k}_2}\Theta^{>}_{\vec{k}_2-\vec{q}}}{E_2(\omega)}\Xi^{C}(\vec{k}_1,-\vec{k}_2;\vec{q},\omega)\,, \tag{20}$$

where $\Xi^{C}=\Xi^{p\text{-}\bar{p}C}+\Xi^{PC}$, and

$$\Xi^{p\text{-}\bar{p}C}(\vec{k}_1,-\vec{k}_2;\vec{q},\omega)=2\langle\vec{q}+\vec{k}\,|\,\Xi^{e\text{-}h}(\vec{K},\omega+\epsilon^{(0)}_{\vec{k}_1}-\epsilon^{(0)}_{\vec{q}-\vec{k}_2})\,|\,\vec{k}\rangle-\langle\vec{q}+\vec{k}\,|\,\Xi^{e\text{-}h}_{ex}(\vec{K},\omega+\epsilon^{(0)}_{\vec{k}_1}-\epsilon^{(0)}_{\vec{q}-\vec{k}_2})\,|\,\vec{k}\rangle\,, \tag{21a}$$

$$\Xi^{PC}(\vec{k}_1,-\vec{k}_2;\vec{q},\omega)=-\tfrac{1}{2}[V(\vec{K})+2\langle\tfrac{1}{2}(\vec{q}+\vec{K})\,|\,\Xi^{P}(\vec{\mathscr{K}},\omega+\epsilon^{(0)}_{\vec{k}_1}-\epsilon^{(0)}_{\vec{q}-\vec{k}_2})\,|\,\tfrac{1}{2}(\vec{q}-\vec{K})\rangle$$
$$-\langle\tfrac{1}{2}(\vec{q}+\vec{K})\,|\,\Xi^{P}_{ex}(\vec{\mathscr{K}},\omega+\epsilon^{(0)}_{\vec{k}_1}-\epsilon^{(0)}_{\vec{q}-\vec{k}_2})\,|\,\tfrac{1}{2}(\vec{q}-\vec{K})\rangle]\,. \tag{21b}$$

The interaction Ξ^{C} has been constructed to include only electron-hole correlations for which there are severe restrictions on the transfer of momentum within the interaction.

As before we display the explicit form of Ξ^{C} through its second-order Born terms:

$$(\Xi^{e\text{-}h}+\Xi^{e\text{-}h}_{ex})^{C}_{2}=\sum_{\vec{p}} V(\vec{q}+\vec{k}-\vec{p})\frac{\Theta^{<}_{-\vec{p}_2,}\Theta^{>}_{\vec{p}_1,}}{E_2(\omega)-\vec{K}\cdot(\vec{p}-\vec{k})}[V(\vec{p}-\vec{k})-\tfrac{1}{2}V(\vec{K})]\,, \tag{22a}$$

$$(\Xi^{P}+\Xi^{P}_{ex})^{C}_{2}=-\tfrac{1}{2}\sum_{\vec{p}} V(\vec{K})\frac{\Theta^{<}_{-\vec{p}_2,}\Theta^{>}_{\vec{p}_1,}}{E_2(\omega)-\vec{K}\cdot(\vec{p}-\vec{k})}[V(\vec{K})-\tfrac{1}{2}V(\vec{p}-\vec{k})]\,. \tag{22b}$$

The Pauli operators in Eqs. (22) restrict the intermediate relative momentum $\vec{p}$ to values less than $2k_F$. The term $\vec{K}\cdot\vec{p}$ in the energy denominators is thus only of order k_F^2. For large momentum transfer $\vec{q}$ in the single-particle region, $q^2/2-qk_F<\omega<q^2/2+qk_F$. The energy denominators are therefore insensitive to the value of $\vec{p}$, and as ω moves through this region the denominators sweep through zero with a functional variation very similar to that of $\chi^{(0)}(\vec{q},\omega)$. As with the class-B terms—and in contrast with the class-A terms—the variation of the interaction factors in the numerators of Eqs. (22) is not closely coupled to the singular behavior of the energy denominators. Only one interaction factor, $V(\vec{p}-\vec{k})$, peaks near the permitted phase-space region; therefore, unlike the class-A terms, there is no sandwiching of the singular energy denominator between two diverging potentials. For this reason no fine structure in ω arises at large $\vec{q}$ from these class-C terms.

Formally, the term Ξ^{PC}_{2} in Eq. (22b) is divergent when the momentum transfer $\vec{K}$ across it goes to zero, because of the presence of the squared factor $V^2(\vec{K})$. Thus we should sum all the Born terms with this particular form, or equivalently, we can work with the dynamically screened interaction $\underline{V}^{sc}$. Figure 7 shows the dynamically screened electron-hole correlation contribution to $\chi^{C}(\vec{q},\omega)$,

$$\chi''^{C}(\vec{q},\omega)=-2\sum_{\vec{k}_1}\frac{\Theta^{<}_{\vec{k}_1}\Theta^{>}_{\vec{q}_1+\vec{k}_1}}{E_1(\omega)}\sum_{\vec{k}_2}\frac{\Theta^{<}_{\vec{k}_2}\Theta^{>}_{\vec{q}-\vec{k}_2}}{E_2(\omega)}\frac{V(\vec{K})}{\epsilon_C(\vec{K},\omega-\epsilon^{(0)}_{\vec{q}-\vec{k}_2}+\epsilon^{(0)}_{\vec{k}_1})}\,. \tag{23}$$

The forward-propagating dielectric response ϵ_C is given in terms of the RPA dynamic structure factor S^{RPA} by

$$[\epsilon_C(\vec{K},\omega-\epsilon^{(0)}_{\vec{q}-\vec{k}_2}+\epsilon^{(0)}_{\vec{k}_1})]^{-1}=1+2V(\vec{K})\int_0^{\infty}\frac{S^{RPA}(\vec{K},\omega')}{\omega-\epsilon^{(0)}_{\vec{q}-\vec{k}_2}+\epsilon^{(0)}_{\vec{k}_1}-\omega'+i\eta}d\omega'\,. \tag{24}$$

When ϵ_C^{-1} is replaced by unity, one obtains the Hartree-Fock particle-hole correlation term. It is well known that terms in the Hartree-Fock model for $\chi^{sc}(\vec{q},\omega)$ lead to a slowly varying ω dependence with no fine-scale features (although there is significant overall relaxation).[12,13]

The complete expression Eq. (23) dynamically screens the Hartree-Fock correlations. Referring to our argument above for the other class-C contributions, we can conclude again that there is no dynamical fine structure in $\chi''^{C}(\vec{q},\omega)$. An explicit numerical calculation confirms this (see Sec. III C).

Finally, we note that the exchange terms $\Xi^{e\text{-}e}_{ex}$ and $\Xi^{h\text{-}h}_{ex}$ of Fig. 8, corresponding to $\Xi^{e\text{-}e}$ and $\Xi^{h\text{-}h}$ [see Eq. (10)], are class-C terms since the configuration of the hole lines in $\Xi^{e\text{-}e}_{ex}$ and electron lines in $\Xi^{h\text{-}h}_{ex}$ constrain the momentum transfer across the $\Xi^{e\text{-}e}_{ex}$ and $\Xi^{h\text{-}h}_{ex}$ interactions to be less than $2k_F$. These two exchange terms are generically related to the dynamically screened $\chi''^{C}(\vec{q},\omega)$ and constitute corrections to the leading order Hartree-Fock term, despite the fact that their direct counterparts $\Xi^{p\text{-}p}$ give contributions to χ^{A}. They make up the lowest-order contributions to a screened interaction series, which when systematically summed should result in a correction to the previously summed dynamically screened contribution $\chi''^{C}(\vec{q},\omega)$, Eq. (23).

4. Class D

Finally, we consider a set of terms contributing to $\Xi^{sc}[G]$ which includes electron-electron scattering mediated by a pair of dynamically screened interactions which overlap in time (see Fig. 9). We omit any explicit discus-

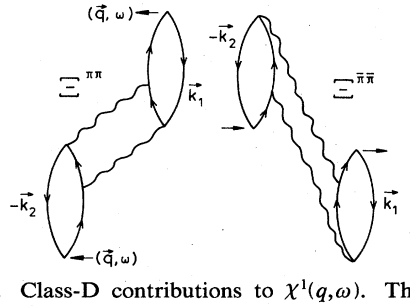

FIG. 9. Class-D contributions to $\chi^{1}(q,\omega)$. The interaction $\Xi^{\pi\pi}$ represents an overlapping two-plasmon excitation propagating forward in time, while $\Xi^{\bar{\pi}\bar{\pi}}$ represents two plasmons propagating backwards.

sion of the corresponding electron-hole and hole-hole class-D contributions merely pointing out that conclusions similar to those in the discussion below can be arrived at for these terms also. One of the time-ordered diagrams, denoted by $\Xi^{\pi\pi}$ in Fig. 9, allows intermediate propagation of two plasmons. However, it is clear from the form of this diagram that the total momentum transported by the plasmon pair is just $\vec{q}$. When $q > 2q_c$, where q_c is the cutoff for a single plasmon, a double resonance will not occur since at least one of the plasmons can readily decay into a single electron-hole pair. On this basis one would not expect to observe a two-plasmon peak in the dynamic structure factor when $q \gtrsim 2q_c$.

In the usual way we write the total contribution to $\chi^1(\vec{q},\omega)$ as

$$\chi^{\mathrm{D}}(\vec{q},\omega)=4\sum_{\vec{k}_1}\frac{\Theta^{<}_{\vec{k}_1}\Theta^{>}_{\vec{q}+\vec{k}_1}}{E_1(\omega)}\sum_{\vec{k}_2}\frac{\Theta^{<}_{\vec{k}_2}\Theta^{>}_{\vec{q}-\vec{k}_2}}{E_2(\omega)}\times\Xi^{\mathrm{D}}(\vec{k}_1,\vec{k}_2;\vec{q},\omega)\ . \tag{25}$$

To make the expression for Ξ^{D} more manageable, we make use of Eqs. (11) and (24) to write

$$\Xi^{\pi\pi}=\sum_{\vec{p}}\Theta^{>}_{\vec{p}_1}\Theta^{>}_{\vec{p}_2}V^2(\vec{Q}_1)V^2(\vec{Q}_2)\int_0^\infty S^{\mathrm{RPA}}(\vec{Q}_1,\omega_1)d\omega_1\int_0^\infty S^{\mathrm{RPA}}(\vec{Q}_2,\omega_2)d\omega_2\times[(\omega-\omega_1-\omega_2+i\eta)(\omega+\epsilon^{(0)}_{\vec{k}_2}-\epsilon^{(0)}_{\vec{p}_2}-\omega_2+i\eta)\times(\omega+\epsilon^{(0)}_{\vec{k}_1}-\epsilon^{(0)}_{\vec{p}_1}-\omega_1+i\eta)]^{-1}\ , \tag{26a}$$

$$\Xi^{\bar{\pi}\bar{\pi}}=\sum_{\vec{p}}\Theta^{>}_{\vec{p}_1}\Theta^{>}_{\vec{p}_2}V^2(\vec{Q}_1)V^2(\vec{Q}_2)\int_0^\infty S^{\mathrm{RPA}}(\vec{Q}_1,\omega_1)d\omega_1\int_0^\infty S^{\mathrm{RPA}}(\vec{Q}_2,\omega_2)d\omega_2\times[(-\omega-\omega_1-\omega_2+i\eta)(\epsilon^{(0)}_{\vec{k}_2}-\epsilon^{(0)}_{\vec{p}_2}-\omega_1+i\eta)\times(\epsilon^{(0)}_{\vec{k}_1}-\epsilon^{(0)}_{\vec{p}_1}-\omega_2+i\eta)]^{-1}\ . \tag{26b}$$

The term $\Xi^{\pi\pi}$ expresses the forward propagation of a correlated plasmon pair. Since the intermediate momenta $\vec{Q}_1$ and $\vec{Q}_2$ sum to $\vec{q}$, the double-plasmon resonance from the combined structure factors $S^{\mathrm{RPA}}(\vec{Q}_1,\omega_1)$ and $S^{\mathrm{RPA}}(\vec{Q}_2,\omega_2)$ disappears when either $\vec{Q}_1$ or $\vec{Q}_2$ moves above the plasmon cutoff q_c. For values of q less than $2q_c$ we would expect resonance effects in $\Xi^{\pi\pi}$ associated with the propagation of two real plasmons.

The term $\Xi^{\bar{\pi}\bar{\pi}}$ represents backward propagation of the intermediate plasmon pair. Its denominator structure shows no singularities for positive values of ω and consequently contributes no fine-scale structure.

B. Self-energies

We now turn to the single-particle self-energy insertions in the dressed propagators $\underline{G}$ of $\chi^{\mathrm{sc}}(\vec{q},\omega)$. While these terms contribute significantly to $\chi^{\mathrm{sc}}(\vec{q},\omega)$, we show that they do not lead to any additional fine-scale dynamical behavior at large momenta, so that in the end it is the electron-electron scattering in $\underline{\Xi}^{\mathrm{A}}[\underline{G}]$ which is the dominating source of the fine-scale energy peaks.

It is well known[7] that there are systematic cancellations between self-energy insertions $\underline{\Sigma}[\underline{G}]$ and particle-hole interaction $\underline{\Xi}^{\mathrm{sc}}[\underline{G}]$. A specific instance of this is the Hartree-Fock model, where it has been shown[11–13] that self-energies and electron-hole correlations in combination are important for determining overall relaxation effects. The cancellation between $\underline{\Sigma}[\underline{G}]$ and $\underline{\Xi}^{\mathrm{sc}}[\underline{G}]$ follows from expanding Eq. (4) for the particle-hole vertex $\underline{\Lambda}^{\mathrm{sc}}[\underline{G}]$ directly in terms of bare propagators $\underline{G}^{(0)}$. Any model satisfying the requirements of Ref. 9 automatically contains this form of cancellation.

Consider the leading term $\chi^0(\vec{q},\omega)$ in the expansion of the proper polarization $\chi^{\mathrm{sc}}(\vec{q},\omega)$ in powers of $\underline{\Xi}^{\mathrm{sc}}[\underline{G}]$, Eq. (6). In principle the single-particle propagator $G(\vec{p},p^0)$ is determined by the self-consistent solution of Eq. (3) expressed as a Dyson equation:

$$G(\vec{p},p^0)=G^{(0)}(\vec{p},p^0)+G^{(0)}(\vec{p},p^0)\{\Sigma[\underline{G}](\vec{p},p^0)\}\times G(\vec{p},p^0)\ . \tag{27}$$

To calculate the dynamical contribution of the self-energy functional $\underline{\Sigma}[\underline{G}]$, as defined by its diagrams (see, e.g., Fig. 10), one should first expand the right-hand side of Eq. (27) in powers of the bare propagator $\underline{G}^{(0)}$:

$$G(\vec{p},p^0)=G^{(0)}(\vec{p},p^0)+G^{(0)}(\vec{p},p^0)\{\Sigma[\underline{G}^{(0)}](\vec{p},p^0)\}\times G^{(0)}(\vec{p},p^0)+\cdots\ , \tag{28}$$

where the truncated terms are of higher order in $\underline{\Sigma}[\underline{G}^{(0)}]$. The zeroth-order contribution to $\chi^0(\vec{q},\omega)$, coming from the replacement of its electron and hole propagators with the bare propagators $\underline{G}^{(0)}$, is just the Lindhard function. The first-order self-energy insertions in $\chi^0(\vec{q},\omega)$ are shown in Fig. 10 as time-ordered diagrams. They are explicitly evaluated in Appendix A [Eqs. (A12) and (A13)].

In each diagram of Fig. 10 an incoming electron or hole is initially excited into an intermediate state by scattering off an electron-hole pair from the background, and relaxes back to its original state after a final interaction. If the

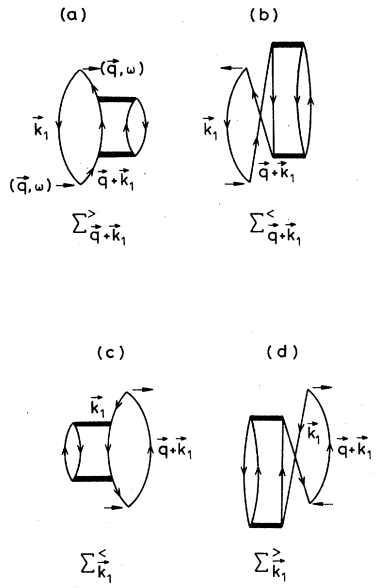

FIG. 10. First-order self-energy insertions in the particle-hole propagator χ^0. (a) and (c) are off-shell contributions which are constrained to propagate only within the lifetime of χ^0. (b) and (d) are on-shell contributions and have no such constraint on their lifetimes.

incoming electron is scattered into a similar intermediate electron (not hole) state, then the amplitude of this self-energy insertion lies off the energy shell. This follows from the restricted lifetime for the scattering, which must take place within the lifetime of $\chi^0(\vec{q},\omega)$. If, however, at any stage the electron is scattered into a hole intermediate state, then the resulting amplitude is on the energy shell because the self-energy lifetime in this case is unrestricted. Similar arguments apply for an incoming hole.

The same lifetime constraints apply to all self-energy insertions in all components of $\chi^{sc}(\vec{q},\omega)$; the fact that there exist off-shell $\lessgtr$ insertions within every electron-hole propagator means that neither the electron nor the hole can be assumed to propagate in total independence of its partner.

In Appendix A we present a more detailed formal discussion of the self-energy structure. Here we simply make use of the general expression for terms such as those of Fig. 10. For an electron with momentum $\vec{q}+\vec{k}_1$ the self-energy $\Sigma^e_{\vec{q}+\vec{k}_1}$ is

$$\Sigma^e_{\vec{q}+\vec{k}_1}\equiv\Sigma^{>}_{\vec{q}+\vec{k}_1}(\omega+\epsilon^{(0)}_{\vec{k}_1}+i\eta)+\Sigma^{<}_{\vec{q}+\vec{k}_1}(\epsilon^{(0)}_{\vec{q}+\vec{k}_1}) , \tag{29}$$

where $\Sigma^{>}$ ($\Sigma^{<}$) denotes intermediate propagation of a particle as an electron (hole). Expressions for $\Sigma^{>}$ and $\Sigma^{<}$ are given in Eqs. (A13). For the hole with momentum $\vec{k}_1$, the self-energy $\Sigma^h_{\vec{k}_1}$ is

$$\Sigma^h_{\vec{k}_1}\equiv\Sigma^{<}_{\vec{k}_1}(\epsilon^{(0)}_{\vec{q}+\vec{k}_1}-\omega-i\eta)+\Sigma^{>}_{\vec{k}_1}(\epsilon^{(0)}_{\vec{k}_1}) . \tag{30}$$

We have shown the explicit energy dependence of each contribution.

To lowest order in Σ the forward-propagating part of $\chi^0(\vec{q},\omega)$ can be written as

$$\chi^0_F(\vec{q},\omega)=\chi^{(0)}_F(\vec{q},\omega)+2\sum_{\vec{k}_1}\frac{\Theta^{<}_{\vec{k}_1}\Theta^{>}_{\vec{q}+\vec{k}_1}}{E_1(\omega)}\times(\Sigma^e_{\vec{q}+\vec{k}_1}-\Sigma^h_{\vec{k}_1})\frac{1}{E_1(\omega)} , \tag{31}$$

where F denotes forward time propagation, and $\chi^{(0)}_F(\vec{q},\omega)$ is the forward-propagating part of the Lindhard function,

$$\chi^{(0)}_F(\vec{q},\omega)\equiv 2\sum_{\vec{k}_1}\frac{\Theta^{<}_{\vec{k}_1}\Theta^{>}_{\vec{q}+\vec{k}_1}}{E_1(\omega)} . \tag{32}$$

[Note that we can recover χ^0 through the relation $\chi^0(\vec{q},\omega)=\chi^0_F(\vec{q},\omega)+\chi^0_F(\vec{q},-\omega)$.]

The completely dressed polarization function $\chi^0_F(\vec{q},\omega)$ can be approximated by inserting in all orders Σ^e and Σ^h into the electron and hole lines of χ^0_F. The result is

$$\chi^0_F(\vec{q},\omega)\approx 2\sum_{\vec{k}_1}\frac{\Theta^{<}_{\vec{k}_1}\Theta^{>}_{\vec{q}+\vec{k}_1}}{E_1(\omega)-\Sigma^e_{\vec{q}+\vec{k}_1}+\Sigma^h_{\vec{k}_1}+i\eta} . \tag{33}$$

Let us look more closely at the structure of the energy denominator in this equation. Using Eqs. (29) and (30), we obtain

$$\begin{aligned}E_1(\omega)-\Sigma^e_{\vec{q}+\vec{k}_1}+\Sigma^h_{\vec{k}_1}&=\omega-[\epsilon^{(0)}_{\vec{q}+\vec{k}_1}+\Sigma^{>}_{\vec{q}+\vec{k}_1}(\omega+\epsilon^{(0)}_{\vec{k}_1})+\Sigma^{>}_{\vec{q}+\vec{k}_1}(\epsilon^{(0)}_{\vec{q}+\vec{k}_1})]+[\epsilon^{(0)}_{\vec{k}_1}+\Sigma^{<}_{\vec{k}_1}(\epsilon^{(0)}_{\vec{q}+\vec{k}_1}-\omega)+\Sigma^{>}_{\vec{k}_1}(\epsilon^{(0)}_{\vec{k}_1})]\\&\equiv\widetilde{E}_1(\omega)-\{\Sigma^{>}_{\vec{q}\,\vec{k}_1}(\epsilon^{(0)}_{\vec{q}+\vec{k}_1}+E_1(\omega))-\Sigma^{>}_{\vec{q}+\vec{k}_1}(\epsilon^{(0)}_{\vec{q}+\vec{k}_1}+i\eta)\}\\&\quad+\{\Sigma^{<}_{\vec{k}_1}(\epsilon^{(0)}_{\vec{k}_1}-E_1(\omega))-\Sigma^{<}_{\vec{k}_1}(\epsilon^{(0)}_{\vec{k}_1}-i\eta)\} ,\end{aligned} \tag{34}$$

where we have introduced the on-shell electron-hole energy

$$\widetilde{E}_1(\omega)=\omega-[\epsilon^{(0)}_{\vec{q}+\vec{k}_1}+\Sigma^{>}_{\vec{q}+\vec{k}_1}(\epsilon^{(0)}_{\vec{q}+\vec{k}_1}+i\eta)+\Sigma^{<}_{\vec{q}+\vec{k}_1}(\epsilon^{(0)}_{\vec{q}+\vec{k}_1})]+[\epsilon^{(0)}_{\vec{k}_1}+\Sigma^{<}_{\vec{k}_1}(\epsilon^{(0)}_{\vec{k}_1}-i\eta)+\Sigma^{>}_{\vec{k}_1}(\epsilon^{(0)}_{\vec{k}_1})]+i\eta , \tag{35}$$

by adding and subtracting the on-shell evaluations of $\Sigma^{>}_{\vec{q}+\vec{k}_1}$ and $\Sigma^{<}_{\vec{k}_1}$ in Eq. (34).

Hedin and Lundqvist, who investigated the energy-dependent properties of the dynamically screened single-particle self-energy,[14] found that the imaginary part of this self-energy on the shell rose sharply to a value of or-

der $\frac{1}{2}E_F^{(0)}$ when the electron's momentum crossed a threshold $\approx 2k_F$, ($|\vec{q}+\vec{k}_1| \approx 2k_F$). If one approximates the energy denominator of Eq. (33) by the expression Eq. (35), using a *purely on-shell* electron self-energy, then the resulting quantity $[-\mathrm{Im}\chi_F^0(\vec{q},\omega)]$ will exhibit a marked peak-and-dip structure around $\omega \approx 2E_F^{(0)}$. This is directly due to the sudden jump of the on-shell self-energy at $|\vec{q}+\vec{k}| \approx 2k_F$. We show in Appendix A that if the *off-shell* self-energy terms are correctly included in the energy denominator of Eq. (33) then only the usual broad peak will be obtained with no anomalous fine structure. It is therefore essential to correctly treat the off-shell contributions to the self-energies in the joint propagation of an electron-hole pair. Consequently we suggest that if the calculations of Mukhopadhyay, Kalia, and Singwi[15] and of Awa, Yasuhara, and Asahi[16] were repeated with the self-energies correctly taken off the energy shell then the twin peak structure they reported for $S(\vec{q},\omega)$ would not appear.

We conclude that neglect of the off-shell contributions to the single-particle self-energy in the joint propagation on an electron-hole pair is unjustified, and furthermore that the consistent inclusion of off-shell effects does not contribute to the fine-scale dynamical structure of $\chi^0(\vec{q},\omega)$ or more generally to the fine-scale structure of $\chi^{sc}(\vec{q},\omega)$ as a whole.

C. Calculational scheme

We have now identified the strongly dynamic and nonlocal part, $\Xi^{e\text{-}e}$, of the two-body interaction Ξ^{sc}. At large momentum transfers $\Xi^{e\text{-}e}$ dominates the contributions $\chi^A(\vec{q},\omega)$ to $\chi^1(\vec{q},\omega)$. The remaining dynamic contribution, $\chi^C(\vec{q},\omega)$, contains the parts of Ξ^{sc} which depend weakly on $(\vec{q},\omega)$ and are approximately local.

Figure 11 illustrates this point for the interactions Ξ^{PC} (Fig. 7) and $\Xi^{e\text{-}eA}$ (Fig. 3) at $q=1.75k_F$ and $r_s=2$. We plot

$$\gamma[\Xi](\vec{q},\omega) = -\frac{[\underline{\Lambda}^{(0)}:\underline{\Xi}:\underline{\Lambda}^{(0)}](\vec{q},\omega)}{\chi_F^{(0)}(\vec{q},\omega)V(\vec{q})\chi_F^{(0)}(\vec{q},\omega)} \tag{36a}$$

for $\Xi=\Xi^{PC}$ and $\Xi=\Xi^{e\text{-}eA}$. The denominator is chosen so that if Ξ is a purely static function then $\gamma[\Xi]$ will be independent of ω. Also plotted is the function $\gamma^{loc}[\Xi](\vec{q},\omega)$ for which the hole propagators in Eq. (36a) have been averaged over (i.e., the usual local average).[3] In this case the $\underline{\Lambda}^{(0)}$ propagators factor out, canceling with the $\chi_F^{(0)}$ and leaving

$$\gamma^{loc}[\Xi](\vec{q},\omega) = -\langle \Xi \rangle_{loc}(\vec{q},\omega)/V(\vec{q}) \; . \tag{36b}$$

Figure 11(a) shows these functions for Ξ^{PC}. The real and imaginary parts are both smoothly varying functions

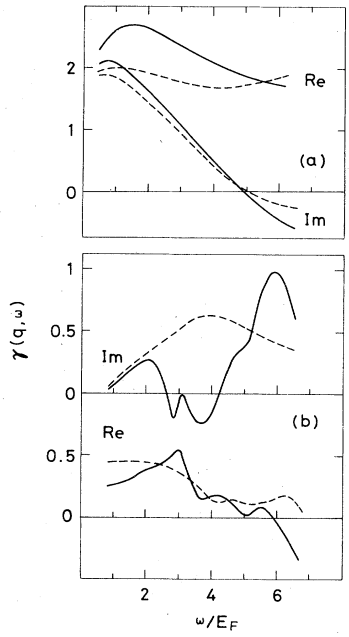

FIG. 11. Approximate local-field factors corresponding to $\chi^1(\vec{q},\omega)$, at $r_s=2$, $q=1.76k_F$. Solid lines: exact factors. Dashed lines: hole-averaged factors. (a) Factors for $\chi'^C(\vec{q},\omega)$. (b) Factors for $\chi^A(\vec{q},\omega)$.

of ω, and γ^{loc} appears to be a good approximation to γ. One should contrast this with the result for $\Xi^{e\text{-}eA}$ shown in Fig. 11(b); real and imaginary parts are here very sensitive to the value of ω, and γ^{loc} does not represent γ at all accurately. The vertical scales in the two plots are different, and we see that the magnitude of $\gamma[\Xi^{PC}]$ is typically much greater than that of $\gamma[\Xi^{e\text{-}eA}]$.

The class-C terms govern the overall relaxation effects in the dynamic response of the correlated electron system. In general these effects are large but dynamically featureless, and we wish to separate the dynamically interesting term $\Xi^{e\text{-}e}$ from these terms. To do this we recall the following procedure from paper I. First we separate Ξ^{sc} into a "nonlocal" part Ξ^{nl} and a "local" part Ξ^{loc} by defining

$$\begin{aligned} \Xi^{nl} &\equiv \Xi^{p\text{-}p} \\ \Xi^{loc} &\equiv \Xi^{sc} - \Xi^{p\text{-}p} \\ &= \Xi^{p\text{-}\bar{p}} + \Xi^{P} + \Xi_{ex}^{p\text{-}\bar{p}} + \Xi_{ex}^{P} + \Xi_{ex}^{p\text{-}p} \; . \end{aligned} \tag{37}$$

Note that Ξ^{loc} is not strictly a local function, but contains those parts of Ξ^{sc} which can be well represented by a local approximation. Our definition of Ξ^{nl} includes hole-hole as well as electron-electron scattering, so that this interaction is time symmetric (as is Ξ^{loc}). It can then be shown[1] that $\chi^{sc}(\vec{q},\omega)$ has an explicit expansion in powers of Ξ^{nl}:

$$\begin{aligned} \chi^{sc}(\vec{q},\omega) = 2\sum_{\vec{k}_1} \int \frac{dk_1^0}{2\pi i} \Lambda^{loc}[\underline{G}](\vec{k}_1,k_1^0;\vec{q},\omega) \\ +4\sum_{\vec{k}_1}\sum_{\vec{k}_2} \int \frac{dk_1^0}{2\pi i} \int \frac{dk_2^0}{2\pi i} \{\Lambda^{loc}[\underline{G}](\vec{k}_1,k_1^0;\vec{q},\omega)\} \\ \times \tfrac{1}{4} \sum_{\sigma_1,\sigma_2} \{\Xi_{\sigma_1\sigma_2}^{nl}[\underline{G}](\vec{k}_1,k_1^0,\vec{k}_2,k_2^0;\vec{q},\omega)\}\{\Lambda^{loc}[\underline{G}](\vec{k}_2,k_2^0;\vec{q},\omega)\} + \cdots \; , \end{aligned} \tag{38}$$

where $\Lambda^{\rm loc}[\underline{G}](\vec{k}_1,k_1^0;\vec{q},\omega)$ satisfies Eq. (4) with $\Xi^{\rm loc}$ replacing $\Xi^{\rm sc}$ (note that $\underline{G}$ remains as before), and the truncated terms are of higher order in $\Xi^{\rm nl}[\underline{G}]$.

Equation (38) is merely a convenient rearrangement of all the contributions to $\chi^{\rm sc}(\vec{q},\omega)$. Let us introduce a dimensionless parameter

$$\alpha=\frac{(-i\underline{G}\underline{G}):\Xi^{\rm nl}[\underline{G}]:(-i\underline{G}\underline{G})/\chi_0}{1-\chi_0\langle\Xi^{\rm loc}\rangle_{\rm loc}} .$$

Provided α is small compared with unity, correction terms of higher order in $\Xi^{\rm nl}$ in Eq. (38) will not contribute significantly and we can truncate the expression after the second term. In Table I we show the value of α for various r_s and $q>k_F$. At high densities $r_s<1$ the parameter α remains small for all $q>k_F$. As the density decreases the lower bound on q for which α remains small increases, so when $r_s=4$ is reached, α remains small only for $q\gtrsim 2k_F$. In the other limit, for small q, all contributions to $\Xi^{\rm sc}$ are of comparable magnitude and share the same functional behavior. In this limit the separation of $\Xi^{\rm sc}$ into local and nonlocal parts no longer serves a useful purpose. In this work we concentrate on the behavior of $\Xi^{\rm nl}$ and $\chi^{\rm sc}(\vec{q},\omega)$ in the range of q for which the parameter α is small.

Our primary aim now is to investigate the dynamical contributions to $\Xi^{\rm nl}$ and the dependence on ω of the nonlocal dynamical part of $\chi^{\rm sc}(\vec{q},\omega)$. For simplicity, in this initial calculation we neglect the relaxation effects residing in the local electron-hole vertex $\Lambda^{\rm loc}$. In this scheme Eq. (38) becomes

$$\chi^{\rm sc}(\vec{q},\omega)\approx\chi^{(0)}(\vec{q},\omega)+\chi^{e\text{-}e\,{\rm A}}(\vec{q},\omega)+\chi^{e\text{-}e\,{\rm A}}(\vec{q},-\omega)+2\chi^{e\text{-}e\,{\rm B}}(\vec{q},\omega) , \quad (39)$$

where $\chi^{e\text{-}e\,{\rm A}}$ is defined by Eq. (7) and $\chi^{e\text{-}e\,{\rm B}}$ by Eq. (14), and we retain only the direct electron-electron pair scattering contribution in $\Xi^{\rm nl}=\Xi^{\rm p\text{-}p}$. Our numerical calculations reported in Sec. IV of the dynamic structure factor $S(\vec{q},\omega)$ [see Eq. (2)] are all direct applications of Eq. (39).

By adopting the approximation in Eq. (39) we have overlooked all relaxation effects from $\chi^{\rm C}(\vec{q},\omega)$ acting together with self-energy insertions into the single-particle lines $\underline{G}$. Each $\underline{G}$ is replaced with the noninteracting $\underline{G}^{(0)}$. In Table II we give lowest-order estimates of the relaxation arising purely from $\chi^{\rm C}(\vec{q},\omega)$. In future work the broad relaxation effects will be combined with the fine-scale effects from strong electron-electron scattering. For the present calculation we emphasize that we have retained all significant fine-scale structure in ω which, however, will appear centered relative to the RPA spectral function instead of being superimposed on the fully relaxed single-particle spectral function.

TABLE II. First-order Hartree-Fock estimates of peak relaxation in $\chi^{(0)}(\vec{q},\omega)+\chi^{1}(\vec{q},\omega)$.

	$\Delta E/E_F$		
q/k_F	$r_s=2$	$r_s=3.2$	$r_s=4$
0.75	0.1	0.2	0.3
1.25	0.5	0.8	0.8
1.75	1.0	1.5	1.5
2.25	1.1	1.7	1.7
2.75	1.1	1.8	1.9
3.5	1.0	1.9	2.2

IV. NUMERICAL RESULTS

We now discuss the results of numerical calculations for the dynamic structure factor $S(\vec{q},\omega)$ using the computational approach described in the preceding section. In Sec. IV A we present $S(\vec{q},\omega)$ for conduction-electron densities corresponding to Li, Be, and Na, calculated for momentum transfers $q\gtrsim 1.5k_F$. We directly compare our $S(\vec{q},\omega)$ with the observed features of $S^{\rm expt}(\vec{q},\omega)$ measured for Be (Ref. 5) and Li (Ref. 6). In Sec. IV B we present our data in a form useful for other numerical applications.

A. Comparison with experiment

In Fig. 12 we display our $S(\vec{q},\omega)$ calculated for $r_s=3.2$, corresponding to the density of Li, together with experimental data of Priftis, Boviatsis, and Vradis[6] for that metal. $S(\vec{q},\omega)$ (calculated) and $S^{\rm expt}(\vec{q},\omega)$ (measured) are plotted as functions of the energy transfer ω at fixed values of the momentum transfer $\vec{q}$. Since this present calculation omits the smoothly varying static local-field contributions plus the related single-particle self-energies, our calculated fine peaks will be positioned with respect to the center of the RPA peak. This should be the basis of any comparison between these calculated values and the experimental data.

At each value of the momentum transfer there is notable correspondence between the fine-ω structure of our $S(\vec{q},\omega)$ and the fine-ω structure of $S^{\rm expt}(\vec{q},\omega)$. We now compare each pair of curves in some detail.

$q=1.80k_F$. A strong peak a at $\omega=2.1E_F$ exists in

TABLE I. Dimensionless parameter α as a function of r_s and q.

	$r_s=2$		$r_s=3.2$		$r_s=4$	
q/k_F	Reα	Imα	Reα	Imα	Reα	Imα
1.25	0.2	0.3	0.2	0.4	0.6	0.5
1.75	0.1	0.1	0.1	0.3	0.4	0.1
2.25	0.06	0.07	0.1	0.2	0.2	0.1
2.75	0.02	0.05	0.1	0.1	0.1	0.1

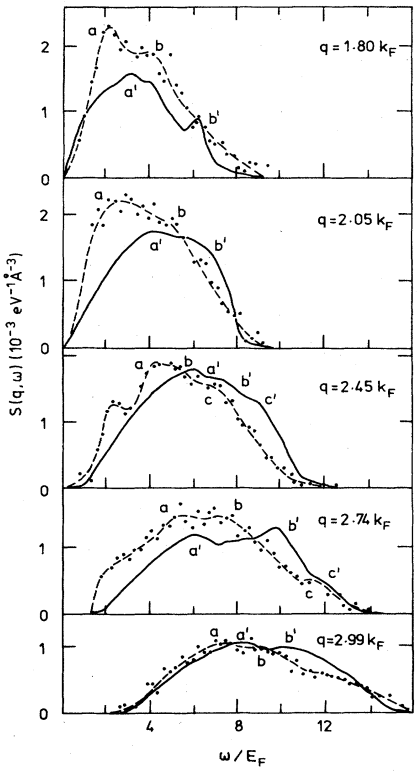

FIG. 12. Dynamic structure factor for Li, at $r_s=3.2$. Solid line: present calculation. Solid circles: x-ray inelastic scattering data points from Ref. 6. Dashed line: guideline from Ref. 6. Absolute energy scale is fixed by $E_F=4.9$ eV. (Our curve for $q=2.05k_F$ is plotted with data measured for $q=2.01k_F$.) The letters a, a', etc. indicate corresponding peaks. In comparing the curves it should be noted that our calculation omits contributions which lead to an overall relaxation $\sim 2E_F$ (cf. Table II).

$S^{\text{expt}}(\vec{q},\omega)$ together with a well-defined shoulder b at $\omega=4E_F$. Correspondingly, $S(\vec{q},\omega)$ has a strong but somewhat broader peak structure a' at $\omega=3.2E_F$ and a sharp dip and peak b' at $\omega=6E_F$. Both curves exhibit pronounced band tails beyond $\omega=7E_F$.

$q=2.05k_F$. The experimental curve has a broad asymmetric maximum a, peaking at $\omega=2.5E_F$, with a shoulder b at $\omega=4.5E_F$. Our calculated curve has a strikingly similar shape, with its peak a' at $\omega=4E_F$ and its shoulder b' at $\omega=6E_F$.

$q=2.45k_F$. At this momentum transfer $S^{\text{expt}}(\vec{q},\omega)$ shows a distinctive low-energy peak at $\omega=2.5E_F$, the suggestion of a twin peak maximum a and b extending from $\omega=4.2E_F$ to $\omega=5.2E_F$, and a shoulder c at $\omega=6.5E_F$. In our corresponding $S(\vec{q},\omega)$ we find no evidence of a low-energy peak. However the steplike sequence of a maximum a' plus two shoulders b' and c' at energies $6E_F$, $7.2E_F$ and $9E_F$ is very similar to the plateau-and-shoulder feature a-b-c in $S^{\text{expt}}(\vec{q},\omega)$.

$q=2.74k_F$ and $q=2.99k_F$. We can identify the peaks a with a' and b with b' for both pairs of curves. At $q=2.74k_F$ we also have a peak c' at $\omega=11.8E_F$ which could possibly be identified with the peak c in $S^{\text{expt}}(\vec{q},\omega)$ at $\omega=11.7E_F$. However, staying with our uniform relaxation construct, we would conclude that matching c to c' is not very convincing. Moreover, the K-electron excitation threshold for Li occurs right at this point ($\omega\approx 11.5E_F$), and this could well contribute to the experimentally observed peak c. There is still evidence of a low-energy peak around $\omega=2.5E_F$ in the experimental data at $q=2.74k_F$, but at $q=2.99k_F$ there is no low-energy peak. In our calculated curves there is no indication of any low-energy peak in this region.

At $q=2.99k_F$ the superimposed fine-peak structure has become less pronounced. This is to be expected since the contributions to $\chi^{(1)}$ become relatively less important for large q. For values of q above $3k_F$ our curves are relatively featureless.

We find no evidence for any many-body mechanism which would generate the low-energy peak around $\omega=2.5E_F$ for $q=2.45k_F$ and $2.74k_F$. A simple two-plasmon excitation can be ruled out on kinematic grounds, since twice the plasmon cutoff momentum is only $\sim 1.3k_F$. Any possible candidate must presumably be band structure related.

A possibility would be the excitation of a single plasmon accompanied by an interband electron transition with umklapp. The reciprocal-lattice vector here is $G\sim 2.3k_F$, so that in the reduced-zone representation $q=2.45k_F$ would become $q\sim 0.15k_F$. Adding the corresponding single-plasmon energy ($\sim 1.6E_F$) to the typical value of the energy gap for Li ($\gtrsim 0.5E_F$) we obtain for the energy of the process $\gtrsim 2.1E_F$. This is close to the actual peak position. The argument is made plausible by the fact that the cutoff for this process would be at $q\sim 3k_F$, and the observed low-energy peak disappears at this momentum. This argument assumes the plasmon carries off almost all the momentum remaining after umklapp.

In Fig. 13 we show our $S(\vec{q},\omega)$ at $r_s=2$ together with the data reported by Platzman and Eisenberger[5] for Be ($r_s=1.9$). Our results for $r_s=2$ were previously reported in a letter.[8] The comparison of the curves for fixed momentum transfer proceeds in a pattern similar to Li. At $q=1.5k_F$ there is a clear correspondence between the pronounced peak a-a' and shoulder b-b' in both curves. Once again as expected, our curve is nearly uniformly displaced upwards in energy $\sim 2E_F$. At $q=1.75k_F$ our peak a' and our main peak b' match up with the observed peak a and main peak b, accompanied again by the uniform energy shift. At $q=2.1k_F$ we see a well-defined structure on the high-energy side of our broad main peak (a'), with a sharp peak (b') at $\omega=6.5E_F$. By contrast, $S^{\text{expt}}(\vec{q},\omega)$ apparently exhibits a change of slope not only at $\omega\approx 5.5E_F$ (b), but also at $\omega\approx 1.5E_F$, which would correspond to a low-energy peak. The main peak (a) at $\omega\approx 3.5E_F$ is somewhat sharper than our main peak (a'). It would be interesting to see if improved experimental resolution revealed additional structural details on either side of the central peak a.

As in the case of Li there is no evidence in our calculated results for any low-energy peak. Repeating our argument concerning an excitation process of a plasmon plus interband transition with umklapp, the corresponding results would suggest a low-energy peak at $\sim 1.8E_F$ existing

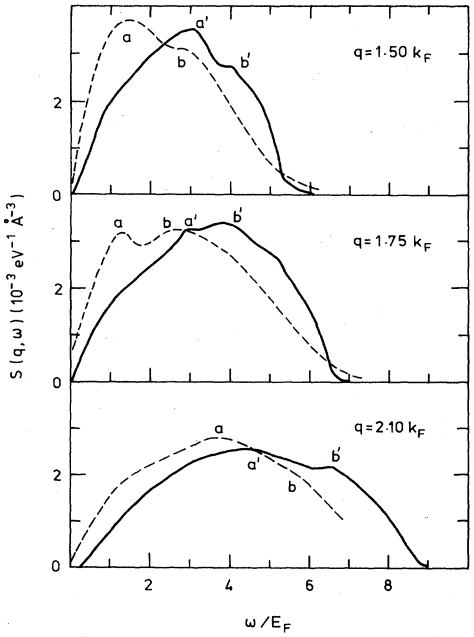

FIG. 13. The dynamic structure factor for Be, at $r_s=2$ ($E_F=12.5$ eV). Solid line: present calculation. Dashed line: x-ray inelastic scattering data from Ref. 5.

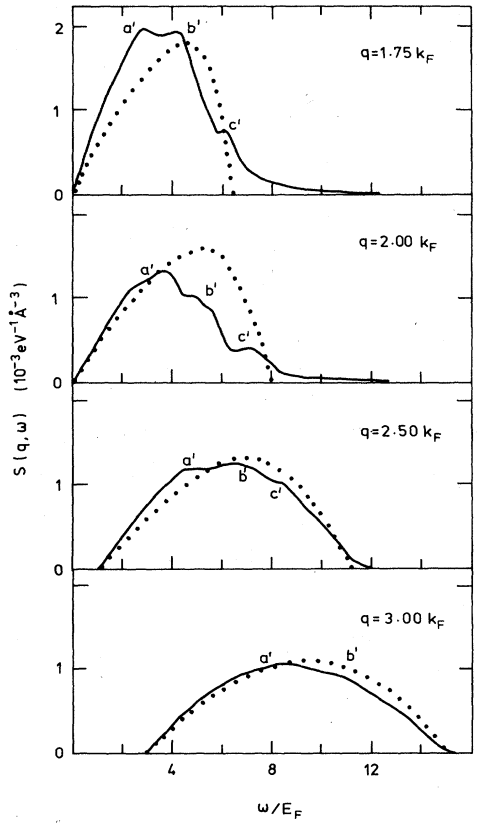

FIG. 14. Dynamic structure factor at $r_s=4$ ($E_F=3.1$ eV) corresponding to Na. Solid line: present calculation. Dotted line: RPA calculation. The overall relaxation of the calculated peaks results from the slowly-varying part of the T-matrix contribution to the local field.

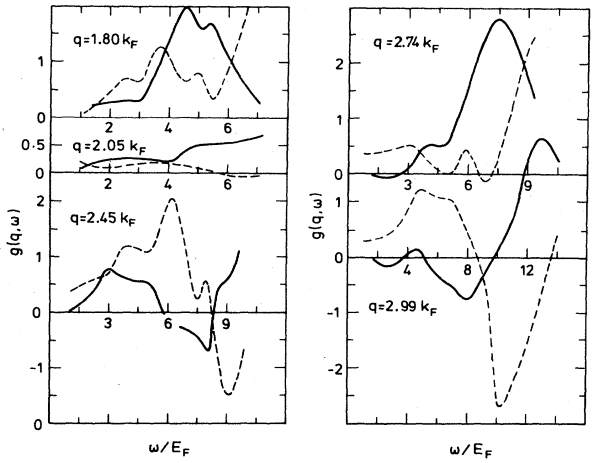

FIG. 15. Nonlocal field factor $g[\underline{\Xi}^{e\text{-}e}](\vec{q},\omega)$, Eq. (36), for density $r_s=3.2$. Dashed lines are the real parts, solid lines the imaginary parts.

only for momentum $0.9k_F \lesssim q \lesssim 2.2k_F$.

Figure 14 shows the structure factor $S(\vec{q},\omega)$ for $r_s=4$. There is unfortunately no published experimental data with which to compare. The dotted curves are the result from RPA and one notes that they are generally less relaxed in energy than our curves. This is consistent with the behavior of the slowly varying T-matrix contributions, which reduce the Coulomb wave-function's amplitude for electron pairs at close range, and as a consequence reduce the electrostatic interaction energy.[3]

B. Nonlocal-field factors

We complete our presentation of numerical results with some data on the effective-field contribution of $\underline{\Xi}^{e\text{-}e}$. In Figs. 15–17 we show the real and imaginary parts of the nonlocal-field factor $g[\underline{\Xi}^{e\text{-}e}](q,\omega)$ at $r_s=3.2$, 2, and 4, where g is defined by

$$g[\underline{\Xi}](\vec{q},\omega)=-\frac{[\underline{\Lambda}^{(0)}:\underline{\Xi}:\underline{\Lambda}^{(0)}](\vec{q},\omega)}{\chi^{(0)}(\vec{q},\omega)V(\vec{q})\chi^{(0)}(\vec{q},\omega)} . \tag{40}$$

The data in Figs. 15–17 may be of use in applications

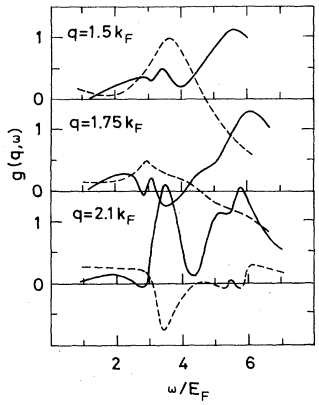

FIG. 16. Nonlocal field factor $g[\underline{\Xi}^{e\text{-}e}](\vec{q},\omega)$ for density $r_s=2$.

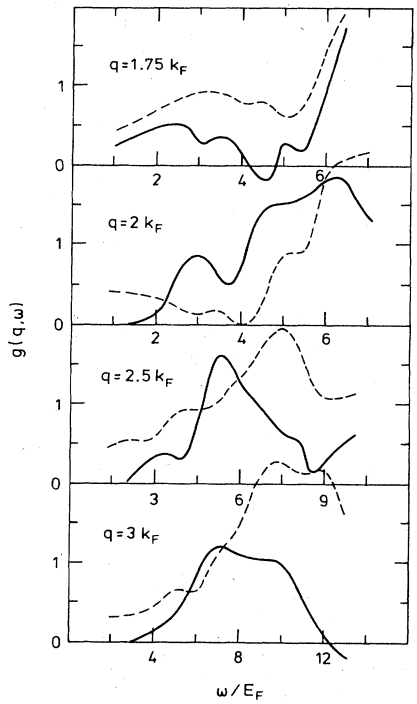

FIG. 17. Nonlocal field factor $g[\underline{\Xi}^{e\text{-}e}](\vec{q},\omega)$ for density $r_s=4$.

requiring estimates of nonlocal effects. However, depending on the application, it would be necessary to exercise care in using these nonlocal-field factors, since the detailed dependence of $\underline{\Xi}$ on the attached electron-hole variables has already been convoluted in our definition of $g[\underline{\Xi}]$.

V. SUMMARY AND CONCLUSION

The purpose of this work was to use our new theory[1] in a practical calculation of dynamical properties of the metallic electron gas. Three main conclusions can be drawn regarding the nature of dynamic correlations in such a system.

(a) Strong Coulomb scattering between electrons dominates the frequency-sensitive contributions to the dynamic structure factor at momentum transfers appreciably larger than the Fermi momentum.

(b) The frequency-sensitive electron-electron scattering contributions are highly nonlocal, in the sense that any averaging of these terms over their internal particle states destroys their detailed frequency dependence. Such averaging is implicit in most mean-field models of correlation effects: It follows that a standard mean-field theory cannot replicate the fine-scale features in the dynamic structure factor.

(c) There is a clear separation, at large momentum transfers, between the rapidly varying nonlocal correlations on the one hand and slowly varying, almost-local correlations on the other. The latter, which are dominated by electron-hole one-pair scattering, are mainly responsible for broad-scale relaxation in the dynamic structure factor. These terms are well approximated by a mean-field construction.

The task of maintaining the conservation laws become quite formidable, once one attempts to treat effects which are inherently dynamical. The nonlocal nature of these effects cannot in general be ignored, and the conservation laws are only satisfied because of cancellations between terms whose functional behavior appears to be disparate. It is a great advantage to adopt a formalism which has the conservation laws already built in it.

The formalism itself is open to further development. One aspect of potential interest to the wider study of Fermi systems concerns the structure of the nonlocal particle-particle scattering effects. It would be useful to establish the extent to which these effects vary with the nature of the particle-particle interaction—for example, if one had a strong short-range potential typical of ^{3}He in place of the Coulomb potential.

APPENDIX A: ELECTRON-HOLE SELF-ENERGIES

In this appendix we determine the functional form of single-particle self-energy insertions when the particle belongs to an electron-hole polarization propagator. We present strong evidence that self-energy insertions, when correctly evaluated off the energy shell, do not contribute any sharp structure to the polarization function.

To simplify the discussion we consider the first-order insertions of $\underline{\Sigma}\equiv\underline{\Sigma}[\underline{G}^{(0)}]$ into the Lindhard function (see, e.g., Fig. 10). For brevity we write $G^{(0)}(p)$ for $G^{(0)}(\vec{p},p^0)$ and $\Sigma(p)$ for $\Sigma[\underline{G}^{(0)}](\vec{p},p^0)$, where $p\equiv(\vec{p},p^0)$; we also set $q\equiv(\vec{q},\omega)$.

The first-order insertions into the electron and hole lines of $\chi^{(0)}(q)$ generate the contribution

$$\chi_1^{(0)}(q)=2\sum_{\vec{k}_1}\int\frac{dk_1^0}{2\pi i}G^{(0)}(k_1)G^{(0)}(q+k_1)[\Sigma(k_1)G^{(0)}(k_1)+\Sigma(q+k_1)G^{(0)}(q+k_1)]\ . \tag{A1}$$

Noting that

$$G^{(0)}(k_1)G^{(0)}(q+k_1)=\frac{1}{E_1(q)}[G^{(0)}(k_1)-G^{(0)}(q+k_1)] \tag{A2}$$

where

$$E_1(q)=\omega-\epsilon^{(0)}_{\vec{q}+\vec{k}_1}+\epsilon^{(0)}_{\vec{k}_1}+i\eta_1\ \ [\eta_1=\eta(\Theta^{<}_{\vec{k}_1}-\Theta^{<}_{\vec{q}+\vec{k}_1})]\ , \tag{A3}$$

Eq. (A1) now splits into two contributions, $\chi_a^{(0)}(q)$ and $\chi_b^{(0)}(q)$:

$$\chi_a^{(0)}(q)=2\sum_{\vec{k}_1}\frac{1}{E_1(q)}\int\frac{dk_1^0}{2\pi i}G^{(0)}(k_1)G^{(0)}(q+k_1)[\Sigma(q+k_1)-\Sigma(k_1)]\ , \tag{A4}$$

$$\chi_b^{(0)}(q)=2\sum_{\vec{k}_1}\frac{1}{E_1(q)}\int\frac{dk_1^0}{2\pi i}\{[G^{(0)}(k_1)]^2\Sigma(k_1)-[G^{(0)}(q+k_1)]^2\Sigma(q+k_1)\}\ . \tag{A5}$$

Again applying Eq. (A2) to $\chi_a^{(0)}(q)$, we have

$$\chi_a^{(0)}(q)=2\sum_{\vec{k}_1}\frac{1}{E_1(q)^2}\int\frac{dk_1^0}{2\pi i}[G^{(0)}(k_1)-G^{(0)}(q+k_1)][\Sigma(q+k_1)-\Sigma(k_1)]\ . \tag{A6}$$

We now evaluate $\chi_1^{(0)}(q)$ using the dynamically screened interaction $\underline{V}^{\rm sc}$ in the self-energy. Specifically

$$\begin{aligned}\Sigma(k)&=-\sum_{\vec{p}}\int\frac{dp^0}{2\pi i}G^{(0)}(k-p)V^{\rm sc}(p)\\&=\Sigma_{\rm HF}(k)-\sum_{\vec{p}}V^2(\vec{p})\int\frac{dp^0}{2\pi i}G^{(0)}(k-p)\int_0^\infty d\omega' S^{\rm RPA}(\vec{p},\omega)\left[\frac{1}{p^0-\omega'+i\eta}-\frac{1}{p^0+\omega'-i\eta}\right].\end{aligned} \tag{A7}$$

Here $\Sigma_{\rm HF}(k)$ is the usual Hartree-Fock self-energy which contributes to $\chi_a^{(0)}(q)$ the term

$$\chi_{\rm HF1}^{(0)}(q)=2\sum_{\vec{k}_1}\frac{\Theta^<_{\vec{k}_1}\Theta^>_{\vec{q}+\vec{k}_1}}{E_1(q)^2}\sum_{\vec{p}}V(\vec{p})(\Theta^<_{\vec{k}_1-\vec{p}}-\Theta^<_{\vec{q}+\vec{k}_1-\vec{p}})\ , \tag{A8}$$

and contributes nothing to $\chi_b^{(0)}(q)$.

For the more interesting dynamical contributions, integration over p^0 gives, from Eq. (A7),

$$\Sigma(k)-\Sigma_{\rm HF}(k)=\sum_{\vec{p}}V^2(\vec{p})\int_0^\infty\frac{S^{\rm RPA}(\vec{p},\omega')}{k^0-\epsilon^{(0)}_{\vec{k}-\vec{p}}-(\Theta^>_{\vec{k}-\vec{p}}-\Theta^<_{\vec{k}-\vec{p}})(\omega'-i\eta)}d\omega'\ . \tag{A9}$$

On substituting into Eq. (A6) we obtain the following products to be integrated over k_1^0:

$$G^{(0)}(k_1)\Sigma(q+k_1)\sim(k_1^0-\epsilon^{(0)}_{\vec{k}_1}-i\eta_1)^{-1}[\omega+k_1^0-\epsilon^{(0)}_{\vec{q}+\vec{k}_1-\vec{p}}-(\Theta^>_{\vec{q}+\vec{k}_1-\vec{p}}-\Theta^<_{\vec{q}+\vec{k}_1-\vec{p}})(\omega'-i\eta)]^{-1}\ , \tag{A10a}$$

$$G^{(0)}(q+k_1)\Sigma(k_1)\sim(\omega+k_1^0-\epsilon^{(0)}_{\vec{q}+\vec{k}_1}+i\eta_1)^{-1}[k_1^0-\epsilon^{(0)}_{\vec{k}_1-\vec{p}}-(\Theta^>_{\vec{k}_1-\vec{p}}-\Theta^<_{\vec{k}_1-\vec{p}})(\omega'-i\eta)]^{-1}\ , \tag{A10b}$$

$$G^{(0)}(k_1)\Sigma(k_1)\sim(k_1^0-\epsilon^{(0)}_{\vec{k}_1}-i\eta_1)^{-1}[k_1^0-\epsilon^{(0)}_{\vec{k}_1-\vec{p}}-(\Theta^>_{\vec{k}_1-\vec{p}}-\Theta^<_{\vec{k}_1-\vec{p}})(\omega'-i\eta)]^{-1}\ , \tag{A11a}$$

$$\begin{aligned}G^{(0)}(q+k_1)\Sigma(q+k_1)\sim&(\omega+k_1^0-\epsilon^{(0)}_{\vec{q}+\vec{k}_1}+i\eta_1)^{-1}\\&\times[\omega+k_1^0-\epsilon^{(0)}_{\vec{q}+\vec{k}_1-\vec{p}}-(\Theta^>_{\vec{q}+\vec{k}_1-\vec{p}}-\Theta^<_{\vec{q}+\vec{k}_1-\vec{p}})(\omega'-i\eta)]^{-1}\ .\end{aligned} \tag{A11b}$$

When $G^{(0)}(k_1)$ propagates as a hole and $G^{(0)}(q+k_1)$ as an electron (forward propagation, $\eta_1=\eta$), the nonvanishing terms give

$$\begin{aligned}\chi_a^{(0)}(q)-\chi_{\rm HF1}^{(0)}(q)=2\sum_{\vec{k}_1}\frac{\Theta^<_{\vec{k}_1}\Theta^>_{\vec{q}+\vec{k}_1}}{E_1(q)^2}&[\Sigma^>_{\vec{q}+\vec{k}_1}(\epsilon^{(0)}_{\vec{k}_1}+\omega)-\Sigma^<_{\vec{k}_1}(\epsilon^{(0)}_{\vec{q}+\vec{k}_1}-\omega)\\&+\Sigma^<_{\vec{q}+\vec{k}_1}(\epsilon^{(0)}_{\vec{q}+\vec{k}_1})-\Sigma^>_{\vec{k}_1}(\epsilon^{(0)}_{\vec{k}_1})]\ ,\end{aligned} \tag{A12}$$

where

$$\Sigma^>_{\vec{k}}(\epsilon)\equiv\sum_{\vec{p}}\Theta^>_{\vec{k}-\vec{p}}V^2(\vec{p})\int_0^\infty\frac{S^{\rm RPA}(\vec{p},\omega')}{\epsilon-\epsilon^{(0)}_{\vec{k}-\vec{p}}-\omega'+i\eta}d\omega'\ , \tag{A13a}$$

$$\Sigma^<_{\vec{k}}(\epsilon)\equiv\sum_{\vec{p}}\Theta^<_{\vec{k}-\vec{p}}V^2(\vec{p})\int_0^\infty\frac{S^{\rm RPA}(\vec{p},\omega')}{\epsilon-\epsilon^{(0)}_{\vec{k}-\vec{p}}+\omega'-i\eta}d\omega'\ . \tag{A13b}$$

Equation (A12) directly demonstrates that there are significant off-energy-shell contributions to the self-energy insertions in a single-particle propagator associated with a particle-hole polarization pair.

For completeness, we also give the contributions to $\chi_b^{(0)}(q)$:

$$\chi_b^{(0)}(q)=-2\sum_{\vec{k}_1}\frac{\Theta^{<}_{\vec{k}_1}\Theta^{>}_{\vec{q}+\vec{k}_1}}{E_1(q)^2}\sum_{\vec{p}}V^2(\vec{p})\int_0^\infty d\omega' S^{\mathrm{RPA}}(\vec{p},\omega')\times\left[\frac{\Theta^{<}_{\vec{q}+\vec{k}_1-\vec{p}}}{(\epsilon^{(0)}_{\vec{q}+\vec{k}_1}-\epsilon^{(0)}_{\vec{q}+\vec{k}_1-\vec{p}}+\omega')^2}+\frac{\Theta^{>}_{\vec{k}_1-\vec{p}}}{(\epsilon^{(0)}_{\vec{k}_1}-\epsilon^{(0)}_{\vec{k}_1-\vec{p}}-\omega')^2}\right]. \tag{A14}$$

Having analyzed the detailed time ordering of self-energy insertions in $\chi^{(0)}(q)$, we now show that such insertions do not change the qualitative shape of the fully renormalized $\chi^0(q)$.

We recall the spectral representation[14] for the single-particle propagator G in terms of $A_{\vec{k}}(\omega')$, the single-particle spectral distribution. We express the polarization function $\chi^0=-i\underline{GG}$ as

$$\chi^0(q)=2\sum_{\vec{k}_1}\int\frac{dk_1^0}{2\pi i}\int d\omega'\frac{A_{\vec{k}_1}(\omega')}{k_1^0-\omega'-i\eta_1}\int d\omega''\frac{A_{\vec{q}+\vec{k}_1}(\omega'')}{\omega+k_1^0-\omega''+i\eta_1}$$

$$=2\sum_{\vec{k}_1}\int d\omega'\int d\omega''\frac{A_{\vec{k}_1}(\omega')A_{\vec{q}+\vec{k}_1}(\omega'')}{\omega-\omega''+\omega'+i\eta_1}\int\frac{dk_1^0}{2\pi i}\left[\frac{1}{k_1^0-\omega'-i\eta_1}-\frac{1}{\omega+k_1^0-\omega''+i\eta_1}\right]. \tag{A15}$$

On evaluating the imaginary part of $\chi^0(q)$ we obtain

$$\mathrm{Im}\chi^0(q)=-2\pi\sum_{\vec{k}_1}\int_{E_F-\omega}^{E_F}A_{\vec{k}_1}(\omega')A_{\vec{q}+\vec{k}_1}(\omega'+\omega)d\omega'. \tag{A16}$$

This equation, which is quite general, demonstrates the intrinsically off-shell character of single-particle self-energy effects in electron-hole polarization contributions such as $\chi^{(0)}(q)$. For the noninteracting case, $A_{\vec{k}}(\omega')=\delta(\omega'-\epsilon^{(0)}_{\vec{k}})$, and the convolution in Eq. (A16) is then reduced to the familiar Lindhard result. When the self-energy of Eq. (A7) is used to define $A_{\vec{k}}(\omega')$, Hedin and Lundqvist[14] have shown that the spectral distribution for electrons ($k>k_F$) retains a sharp single peak at the quasiparticle energy $\epsilon_{\vec{k}}$ while that for holes ($k<k_F$) can develop multiple peaks. Hence, to estimate the effect of the self-energies on the renormalized polarization function $\chi^0(q)$, let us assume a spectral distribution function which has one δ-like peak for electrons and, for example, two peaks, separated by $\Delta\epsilon_{\vec{k}_1}$, for holes:

$$A_{\vec{q}+\vec{k}_1}(\omega+\omega')\approx\delta(\omega'+\omega-\epsilon_{\vec{q}+\vec{k}_1}),$$

$$A_{\vec{k}_1}(\omega')\approx Z_{\vec{k}_1}\delta(\omega'-\epsilon_{\vec{k}_1})+(1-Z_{\vec{k}_1})\delta(\omega'-\epsilon_{\vec{k}_1}-\Delta\epsilon_{\vec{k}_1}). \tag{A17}$$

On substituting into Eq. (A16) we get

$$\mathrm{Im}\chi^0(q)\approx-2\pi\sum_{\vec{k}_1}\Theta^{<}_{\vec{k}_1}\Theta^{>}_{\vec{q}+\vec{k}_1}\times[Z_{\vec{k}_1}\delta(\omega-\epsilon_{\vec{q}+\vec{k}_1}+\epsilon_{\vec{k}_1})+(1-Z_{\vec{k}_1})\delta(\omega+\Delta\epsilon_{\vec{k}_1}-\epsilon_{\vec{q}+\vec{k}_1}+\epsilon_{\vec{k}_1})]. \tag{A18}$$

Equation (A18) represents a superposition of Lindhard-like functions on a broad characteristic scale of order qk_F. Consequently this expression cannot give rise to sharp features in $\chi^0(q)$ on a scale of k_F^2 or less. A broad distribution of this kind for $\chi^0(q)$ follows naturally from the convolution structure of Eq. (A16).

APPENDIX B: CONVOLUTION INTEGRAL FOR χ^1

We present here a general method for calculating a given contribution to $\chi^1(\vec{q},\omega)$ for all $\vec{q}$ and ω. We note that explicit calculations of the Hartree-Fock contribution to $\chi^1(\vec{q},\omega)$ have been published by Geldart and Taylor[17] for the static case ($\omega=0$), and by Holas, Aravind, and Singwi[12] for general values of ω.

For definiteness we treat the contribution $\chi^{\mathrm{A}}(\vec{q},\omega)$. Recalling Eq. (7) we rewrite it as

$$\chi^{\mathrm{A}}(\vec{q},\omega)=4\sum_{\vec{k}_1}\Theta^{<}_{\vec{k}_1}\Theta^{>}_{\vec{q}+\vec{k}_1}\sum_{\vec{k}_2}\Theta^{<}_{\vec{k}_2}\Theta^{>}_{\vec{q}-\vec{k}_2}\frac{1}{E_1(\omega)+E_2(\omega)}\left[\frac{1}{E_1(\omega)}+\frac{1}{E_2(\omega)}\right]\Xi^{A}(\vec{k}_1,-\vec{k}_2;\vec{q},\omega)$$

$$=2\sum_{\vec{k}_1}\sum_{\vec{k}_2}\frac{Q^{<}Q^{>}}{\frac{1}{2}E_1(\omega)[E_1(\omega)+E_2(\omega)]}\Xi^{\mathrm{A}}(\vec{k}_1,-\vec{k}_2;q,\omega), \tag{B1}$$

where we have defined $Q^{<}\equiv\Theta^{<}_{\vec{k}_1}\Theta^{<}_{\vec{k}_2}$ and $Q^{>}\equiv\Theta^{>}_{\vec{q}+\vec{k}_1}\Theta^{>}_{\vec{q}-\vec{k}_2}$; in the second line we have used the symmetry of $Q^{<}$, $Q^{>}$, and Ξ^{A} under the transformation $\vec{k}_1\rightleftarrows-\vec{k}_2$. On converting the sums over $\vec{k}_1$ and $\vec{k}_2$ to integrals, Eq. (B1) becomes

$$\chi^{A}(\vec{q},\omega)=\frac{1}{8\pi^5}\int_0^{k_F}dk\,k^2\int_0^{2k_F}dK\,K^2\int_{-1}^{1}dz\int_{-1}^{1}du\int_0^{\pi}d\phi\,\frac{\Theta(\bar{Q}^{<}-|u_h|)\Theta(\bar{Q}^{>}-|u_e|)\Xi^{A}(\vec{k}_1,-\vec{k}_2;\vec{q},\omega)}{(\omega-\frac{1}{2}q^2-\vec{q}\cdot\vec{k}+i\eta)(\omega-\frac{1}{2}q^2-\vec{q}\cdot\vec{k}-\frac{1}{2}\vec{q}\cdot\vec{K}+i\eta)}\,. \tag{B2}$$

The cosine variables u_h and u_e are defined in terms of $z=\hat{q}\cdot\hat{k}$ and $u=\hat{q}\cdot\hat{K}$, and the azimuth angle ϕ:

$$\begin{aligned}u_h&=uz+[(1-u^2)(1-z^2)]^{1/2}\cos\phi\\ u_e&=(qu+ku_h)/|\vec{q}+\vec{k}|\,,\end{aligned} \tag{B3}$$

where $|\vec{q}+\vec{k}|^2=q^2+k^2+2qkz$. The functions $\bar{Q}^{<}$ and $\bar{Q}^{>}$ are given by

$$\begin{aligned}\bar{Q}^{<}&=\Theta(k_F^2-k^2-\tfrac{1}{4}K^2)\min[1,(k_F^2-k^2-\tfrac{1}{4}K^2)/kK]\,,\\ \bar{Q}^{>}&=\Theta(|\vec{q}+\vec{k}|^2+\tfrac{1}{4}K^2-k_F^2)\min[1,(|\vec{q}+\vec{k}|^2+\tfrac{1}{4}K^2-k_F^2)/|\vec{q}+\vec{k}|K]\,.\end{aligned} \tag{B4}$$

Next we reduce Eq. (B2) to the form

$$\chi^{A}(\vec{q},\omega)=\frac{1}{8\pi^5q^2}\int_0^{k_F}dk\,k\int_{z_c}^{1}dz\frac{1}{z-z_0-i\eta}\int_{K_1}^{K_u}dK\,K\int_{-u_b}^{u_b}du\frac{1}{u-u_0-i\eta}\int_{\phi_1}^{\phi_u}d\phi\,\Xi^{A}(\vec{k}_1,-\vec{k}_2;\vec{q},\omega)\,, \tag{B5}$$

where $z_0=(\omega-q^2/2)/qk$, $u_0=(2\omega-q^2-2kqz)/qK$, and the bounds $z_c,K_u,K_1,u_b,\phi_u,\phi_1$ are rather intricate functions defined as follows:

$$z_c=-\min(1,q/2k)\,, \tag{B6a}$$

$$\begin{aligned}K_u&=2(k_F^2-k^2)^{1/2}\,,\\ K_1&=2[\max(0,k_F^2-k^2-q^2-2qkz)]^{1/2}\,,\end{aligned} \tag{B6b}$$

$$u_b=\min(u_1,u_2,u_3)\,, \tag{B6c}$$

where

$$\begin{aligned}u_1&=(q+2kz)/K\,,\\ u_2&=\Theta(\bar{Q}^{<}-|z|)\\ &\quad+\Theta(|z|-\bar{Q}^{<})(\bar{Q}^{<}|z|+\{[1-(\bar{Q}^{<})^2](1-z^2)\}^{1/2})\,,\\ u_3&=\Theta(\bar{Q}^{>}-|\gamma|)\\ &\quad+\theta(|\gamma|-\bar{Q}^{>})(\bar{Q}^{>}|\gamma|+\{[1-(\bar{Q}^{>})^2](1-\gamma^2)\}^{1/2})\,,\\ \gamma&=(q+kz)(q^2+k^2+2qkz)^{-1/2}\,,\end{aligned}$$

and finally

$$\begin{aligned}\phi_u&=\pi-\cos^{-1}[\min(1,A^-,B^-)]\,,\\ \phi_1&=\cos^{-1}[\min(1,A^+,B^+)]\,,\end{aligned} \tag{B6d}$$

where

$$\begin{aligned}A^{\pm}&=\max\{-1,(\bar{Q}^{>}\pm|\gamma u|)[(1-u^2)(1-\gamma^2)]^{-1/2}\}\,,\\ B^{\pm}&=\max\{-1,(\bar{Q}^{<}\pm|zu|)[(1-u^2)(1-z^2)]^{-1/2}\}\,.\end{aligned}$$

For numerical stability it is essential that these bounds be specified exactly, since from Eq. (B5) it is clear that endpoint singularities can arise from the energy denominators. Given a knowledge of the bounds, the singularities may be treated by standard numerical techniques. We find that the particular order of integration shown in Eq. (B5) is the most efficient for obtaining stable results.

Note that Eqs. (B5) and (B6a) through (B6d) are also applicable to $\chi^{B}(\vec{q},\omega)$. In this case we let $z_0=q/2k$, and for the expression $(u-u_0-i\eta)^{-1}$ in the integration over u we substitute

$$\tfrac{1}{2}\{(u-u_0-i\eta)^{-1}+[u-u_0+4\omega/(qK)-i\eta]^{-1}\}\,. \tag{B7}$$

APPENDIX C: NUMERICAL SOLUTION OF $\Xi^{e\text{-}e}$

We give here some details of the computation of the electron-electron scattering amplitude $\Xi^{e\text{-}e}$. At large momentum transfers the amplitude $\Xi^{e\text{-}e}$ is given by the all-order sum of T-matrix ladders [see Fig. 2(a)]. Specifically we have

$$\langle\vec{p}_2|\Xi^{e\text{-}e}(\vec{P},E)|\vec{p}_1\rangle\equiv\langle\vec{p}_2|T(\vec{P},E)|\vec{p}_1\rangle-V(\vec{p}_2-\vec{p}_1)\,, \tag{C1}$$

where T satisfies the Bethe-Goldstone equation:[18]

$$\begin{aligned}\langle\vec{p}_2|T(\vec{P},E)|\vec{p}_1\rangle&=V(\vec{p}_2-\vec{p}_1)\\ &\quad+\sum_{\vec{p}}V(\vec{p}_2-\vec{p})\frac{Q^{>}(\vec{p},\vec{P},k_F)}{E-\frac{1}{4}P^2-p^2+i\eta}\\ &\quad\times\langle\vec{p}|T(\vec{P},E)|\vec{p}_1\rangle\,.\end{aligned} \tag{C2}$$

Here $Q^{>}(\vec{p},\vec{P},k_F)=\Theta^{>}_{\vec{P}-\vec{p}/2}\Theta^{>}_{\vec{P}+\vec{p}/2}$ is the Pauli projection operator. We will solve Eq. (C2) with $Q^{>}(\vec{p},\vec{P},k_F)$ replaced by its angular average with respect to $\hat{P}\cdot\hat{p}$, i.e.,

$$\bar{Q}^{>}(p,P,k_F)=\Theta(p^2+\tfrac{1}{4}P^2-k_F^2) \times\min[1,(p^2+\tfrac{1}{4}P^2-k_F^2)/pP] . \quad \text{(C3)}$$

The approximation of $Q^{>}$ by its angle average results in an overestimate of $\Xi^{e\text{-}e}$, since it permits partial inclusion of singular contributions from the first and last V in each ladder term of the T matrix. For the exact $Q^{>}$ these contributions are excluded. There is no effect on the qualitative behavior of $\Xi^{e\text{-}e}$, and quantitatively the modifications are only minor.

With the substitution of $\bar{Q}^{>}\approx Q^{>}$ in Eq. (C2), the equation decouples into a set of integral equations for the partial-wave components of the approximate T:

$$t_l(p_2,p_1;P,E)=v_l(p_2,p_1) +\frac{2}{\pi}\int dp\, p^2 v_l(p_2,p)\frac{\bar{Q}^{>}(p,P,k_F)}{E-\frac{1}{4}-P^2-p^2+i\eta} \times t_l(p,p_1;P,E) , \quad \text{(C4)}$$

where the partial-wave components v_l and t_l determine V and T through the expressions

$$V(\vec{p}_2-\vec{p}_1)=4\pi\sum_{l=0}^{\infty}(2l+1)v_l(p_2,p_1)P_l(\hat{p}_2\cdot\hat{p}_1) , \quad \text{(C5)}$$

$$\langle\vec{p}_2\,|\,T(P,E)\,|\,\vec{p}_1\rangle=4\pi\sum_{l=0}^{\infty}(2l+1)t_l(p_2,p_1;P,E) \times P_l(\hat{p}_2\cdot\hat{p}_1) .$$

Here $P_l(x)$ is the Legendre polynomial of order l. Each component v_l of the Coulomb potential is given explicitly in terms of $Q_l(x)$, the Legendre function of the second kind:

$$v_l(p_2,p_1)=\lim_{\mu\to 0}\frac{4\pi e^2}{2p_1p_2}Q_l\left[\frac{p_1^2+p_2^2+\mu^2}{2p_1p_2}\right] . \quad \text{(C6)}$$

The partial-wave equation (C4) for $l=0,1,2,\ldots$ can now be solved systematically. For amplitudes $t_l(p_2,p_1;P,E)$ in which E is below the threshold for real scattering, Eq. (C4) is a regular Fredholm equation and may be solved by standard numerical methods. When t_l corresponds to dynamic scattering (as in $\Xi^{e\text{-}e\,A}$), the energy denominator in Eq. (C4) vanishes when $p^2=p_0^2\equiv E-\frac{1}{4}P^2>0$, and the integral equation is singular. In this case we use a technique due to Kowalski.[19]

Introduce the functions

$$f_l(p_2,p_1)=v_l(p_2,p_1)/v_l(p_0,p_0) , \quad \text{(C7)}$$
$$g_l(p_2,p_1)=t_l(p_2,p_1;P,E)/t_l(p_0,p_0;P,E) .$$

As a function of p_2 for fixed p_0, the function $g_l(p_2,p_0)$ obeys the regular Fredholm equation

$$g_l(p_2,p_0)=f_l(p_2,p_0)+\frac{2}{\pi}\int_0^{\infty}dp\, p^2K_l(p_2,p)\bar{Q}^{>}(p,P,k_F) \times g_l(p,p_0) , \quad \text{(C8)}$$

where the kernel $K_l(p_2,p)$ is defined as

$$K_l(p_2,p)\equiv[v_l(p_2,p)-v_l(p_2,p_0)f_l(p_0,p)](p_0^2-p^2)^{-1} . \quad \text{(C9)}$$

The singularity due to the denominator at $p=p_0$ has been thus removed. However, for a long-ranged potential such as V the numerator diverges at $p=p_0$. We overcome this by introducing a very small but finite convergence factor μ into the Coulomb amplitudes [cf. Eq. (C6)]. Providing μ is sufficiently small our results are insensitive to its value.

The fully on-shell amplitude $t_l(p_0,p_0;P,E)$ can be recovered from the solution $g_l(p,p_0)$ to Eq. (C8) by means of the relations

$$t_l(p_0,p_0;P,E)=\frac{r_l(p_0,p_0)-ip_0\bar{Q}^{>}(p_0,P,k_F)r_l^2(p_0,p_0)}{1+[p_0\bar{Q}^{>}(p_0,P,k_F)r_l(p_0,p_0)]^2} , \quad \text{(C10)}$$

$$r_l(p_0,p_0)=v_l(p_0,p_0)\left[1-\frac{2}{\pi}\int_0^{\infty}dp\frac{1}{p_0^2-p^2}[p^2Q^{>}(p,P,k_F)v_l(p_0,p)g_l(p,p_0)-p_0^2\bar{Q}^{>}(p_0,P,k_F)v_l(p_0,p_0)]\right]^{-1} . \quad \text{(C11)}$$

To obtain the full solution for $t_l(p_1,p_2;P,E)$ when $p_1\neq p_0\neq p_2$, we must extend Eq. (C8) completely off the energy shell. We first solve the fully off-shell equation

$$g_l(p_2,p_1)=v_l(p_2,p_1)+\frac{2}{\pi}\int_0^{\infty}dp\, p^2K_l(p_2,p)\bar{Q}^{>}(p,P,k_F)g_l(p,p_1) . \quad \text{(C12)}$$

The matrix element $t_l(p_2,p_1;P,E)$ is generated from the relation

$$t_l(p_2,p_1;P,E)=g_l(p_2,p_0)t_l(p_0,p_0;P,E)g_l(p_1,p_0) +g_l(p_2,p_1)v_l(p_0,p_0) -v_l(p_2,p_0)g_l(p_1,p_0) . \quad \text{(C13)}$$

We may now solve Eqs. (C8) and (C12) numerically on a discrete mesh of p_1 and p_2 for an appropriate range of the parameters l, P, and $E=p_0^2+\frac{1}{4}P^2$. If $E-\frac{1}{4}P^2$ is positive, the equations are singular and the mesh must be chosen to cluster about $p_0=(E-\frac{1}{4}P^2)^{1/2}$, with a density $\sim p_0/\mu$ to properly take account of the rapid variation of

$K_l(p,p_0)$ in that region. We have found in practice that the first four partial waves are sufficient to guarantee an overall convergence of the partial-wave sum for T to within a few percent in all our calculations.

For class-A terms the following correspondence of variables applies [cf. Eqs. (10) and (B2)]:

$$\begin{aligned}
&\mathcal{K}=(q^2+4k^2+4qkz)^{1/2} \leftrightarrow P \ , \\
&E=\omega+k^2+\tfrac{1}{4}K^2 \leftrightarrow p_0^2+\tfrac{1}{4}P^2 \ , \\
&\tfrac{1}{2}\,|\,\vec{\mathrm{K}}+\vec{\mathrm{q}}\,|=\tfrac{1}{2}(K^2+q^2+2Kqu)^{1/2} \leftrightarrow p_2 \ , \\
&\tfrac{1}{2}\,|\,\vec{\mathrm{K}}-\vec{\mathrm{q}}\,|=\tfrac{1}{2}(K^2+q^2-2Kqu)^{1/2} \leftrightarrow p_1 \ .
\end{aligned} \tag{C14}$$

We can now reconstruct $\Xi^{e\text{-}e\ \mathrm{A}}(\vec{\mathrm{k}}_1,-\vec{\mathrm{k}}_2;\vec{\mathrm{q}},\omega)$:

$$\langle \vec{\mathrm{p}}_2\,|\,\Xi^{e\text{-}e}(\vec{\mathrm{P}},E)\,|\,\vec{\mathrm{p}}_1\rangle=4\pi\sum_{l=0}^{\infty}(2l+1)v_l(p_2,p_1) \times F(l,P,E;p_2,p_1)P_l(\hat{p}_1\cdot\hat{p}_2) \tag{C15}$$

where

$$F(l,P,E;p_2,p_1)=t_l(p_2,p_1;P,E)/v_l(p_2,p_1)-1 \ .$$

While this calculation is somewhat intricate, the computational effort required in strict terms of machine storage and execution time is modest in relation to, for example, typical band-structure calculations.

*Formerly D. N. Lowy.

[1]F. Green, D. Neilson, and J. Szymański, preceding paper, Phys. Rev. B **31**, 2779 (1985).

[2]D. Pines and P. Nozières, *The Theory of Quantum Liquids* (Benjamin, New York, 1966).

[3]D. N. Lowy and G. E. Brown, Phys. Rev. B **12**, 2138 (1975).

[4]D. J. W. Geldart and S. H. Vosko, Can. J. Phys. **44**, 2137 (1966).

[5]P. M. Platzman and P. Eisenberger, Phys. Rev. Lett. **33**, 152 (1974).

[6]G. D. Priftis, J. Boviatsis, and A. Vradis, Phys. Lett. **68A**, 482 (1978).

[7]K. S. Singwi and M. P. Tosi, in *Solid State Physics,* edited by H. Ehrenreich, F. Seitz, and D. Turnbull (Academic, New York, 1981), Vol. 36, p. 177.

[8]F. Green, D. N. Lowy, and J. Szymański, Phys. Rev. Lett. **48**, 638 (1982).

[9]G. Baym and L. P. Kadanoff, Phys. Rev. **124**, 287 (1961); G. Baym, *ibid.* **127**, 1391 (1962).

[10]G. E. Brown, *Many-Body Problems* (North-Holland, Amsterdam, 1972).

[11]D. J. W. Geldart and R. Taylor, Can. J. Phys. **48**, 167 (1970).

[12]A. Holas, P. K. Aravind, and K. S. Singwi, Phys. Rev. B **20**, 4912 (1979).

[13]M. W. C. Dharma-wardana and P. Taylor, J. Phys. F **10**, 2217 (1980).

[14]L. Hedin and S. Lundqvist, in *Solid State Physics,* edited by F. Seitz, D. Turnbull, and H. Ehrenreich (Academic, New York, 1969), Vol. 23, p. 1.

[15]G. Mukhopadhyay, R. K. Kalia, and K. S. Singwi, Phys. Rev. Lett. **34**, 950 (1975).

[16]K. Awa, H. Yasuhara, and T. Asahi, Phys. Rev. B **25**, 3670 (1982); **25**, 3687 (1982).

[17]D. J. W. Geldart and R. Taylor, Can. J. Phys. **48**, 155 (1970).

[18]A. L. Fetter and J. D. Walecka, *Quantum Theory of Many-Particle Systems* (McGraw-Hill, New York, 1971), Chap. 11.

[19]K. L. Kowalski, Phys. Rev. Lett. **15**, 798 (1965).